

Hybrid quantum-classical and quantum-inspired classical algorithms for solving banded circulant linear systems

Po-Wei Huang,^{*} Xiufan Li,[†] Kelvin Koor,[‡] and Patrick Reberstrost[§]

Centre for Quantum Technologies, National University of Singapore, 3 Science Drive 2, Singapore 117543

(Dated: September 21, 2023)

Solving linear systems is of great importance in numerous fields. In particular, circulant systems are especially valuable for efficiently finding numerical solutions to physics-related differential equations. Current quantum algorithms like HHL or variational methods are either resource-intensive or may fail to find a solution. We present an efficient algorithm based on convex optimization of combinations of quantum states to solve for banded circulant linear systems whose non-zero terms are within distance K of the main diagonal. By decomposing banded circulant matrices into cyclic permutations, our approach produces approximate solutions to such systems with a combination of quantum states linear to K , significantly improving over previous convergence guarantees, which require quantum states exponential to K . We propose a hybrid quantum-classical algorithm using the Hadamard test and the quantum Fourier transform as subroutines and show its **PromiseBQP**-hardness. Additionally, we introduce a quantum-inspired algorithm with similar performance given sample and query access. We validate our methods with classical simulations and actual IBM quantum computer implementation, showcasing their applicability for solving physical problems such as heat transfer.

I. INTRODUCTION

Quantum algorithms have been discussed in finding approximate solutions to linear systems of equations. Harrow *et al.* [1] famously gave an efficient quantum algorithm to prepare solutions to sparse, well-conditioned linear systems. However, the HHL algorithm consumes a large amount of quantum resources and may not be useful before fault-tolerant quantum computers are well established. Additionally, variational methods [2, 3] such as the variational quantum linear solver (VQLS) [4] are shown to be executable on noisy intermediate-scale quantum (NISQ) devices [5] but suffers from the barren plateau problem [6] as well as a lack of performance guarantees. To address these problems, Huang *et al.* [7] proposed a near-term solution that utilizes *classical combinations of quantum states* (CQS) and an Ansatz tree to provide a theoretical guarantee of finding the approximate solution with a limited amount of quantum resources. On the other hand, quantum-inspired classical algorithms that utilizes sample and query access [8] to achieve approximate solutions whose performance can potentially match quantum algorithms have also been discussed for finding approximate solutions for linear systems [9–13].

Solving circulant linear systems is a fundamental problem in numerous fields such as modeling physical systems, signal processing, and image reconstruction. Owing to their special properties, state-of-the-art classical algorithms often rely on the fast Fourier transform algorithm (FFT) to diagonalize such matrices [14] and obtain the solution of N -dimensional linear systems using $\mathcal{O}(N \log N)$ operations [15], providing a significant speedup over exact solutions of linear systems such as Gaussian elimination, which may take up to $\mathcal{O}(N^3)$ operations. Further, it may also be faster than approximate solutions for ill-conditioned matrices, such as the conjugate gradient method which takes up to $\mathcal{O}(N\kappa)$ operations [16], where κ is the condition number of the linear system. Given the unique properties of circulant matrices and the close relationship between circulant systems and the discrete Fourier transform (DFT), it is interesting to see what further speedups could be achieved by utilizing the quantum Fourier transform (QFT) [17] to solve circulant systems via quantum algorithms. Zhou and Wang [18] showed an efficient implementation of circulant matrices through unitary decomposition and QFT, allowing the problem to be solved by HHL algorithm. Wan *et al.* [19] on the other hand, directly constructed the inverse of the circulant matrix by diagonalizing with QFT and employing amplitude amplification [20] to invert all eigenvalues.

In this work, we propose an efficient algorithm for solving circulant linear systems by studying the properties of circulant matrices. Following Huang *et al.* [7], instead of explicitly diagonalizing the matrix with DFT, we first decompose the circulant matrix into a sum of cyclic permutation operators. These operators can then be diagonalized individually by DFT. Using QFT in our algorithm requires quantum hardware slightly beyond the capacities of current near-term systems [21]. Our theoretical results show that such a decomposition provides a much tighter upper bound

^{*} huangpowei22@u.nus.edu

[†] lixiufan@u.nus.edu

[‡] cqtjkjk@nus.edu.sg

[§] cqtfr@nus.edu.sg

for convergence guarantees, allowing an experimentally achievable guarantee without invoking gradient expansion Ansatz trees and other heuristical methods, or additional regularization such as Tikhonov regularized regression on the solution vector. This gives rise to a hybrid quantum-classical algorithm that consumes one additional ancilla qubit via Hadamard test [22] to achieve fast inner product estimation.

Alternatively, noting that circulant matrices are simply weighted sums of cyclic permutation operators, we propose a quantum-inspired classical algorithm that uses sample and query access [8] to achieve the same performance as the hybrid algorithm. When cyclic permutation operators are applied to a vector, sample and query access to the original vector suffices to achieve the same access to the permuted vector as only a shift of indexes is required.

The efficacy of our algorithms is demonstrated through numerical solutions¹ to one-dimensional time-dependent heat transfer problems discretized by finite difference methods [23, 24]. Through classical simulations, we show that both the hybrid algorithm and the quantum-inspired algorithm provide decent approximations to exact solutions obtained by matrix multiplications. Furthermore, we implement the hybrid algorithm on IBM quantum hardware with an error of less than 0.05 in terms of the mean-square-error (MSE) loss, showcasing the feasibility of solving physical problems on practical quantum computers.

II. PRELIMINARIES

Notations. Let $[n] := \{0, 1, \dots, n-1\}$ indicate the range of integers from 0 to $n-1$. Let $[a..b]$ be the range of integers from a to b , inclusive of endpoints.

Given a field \mathbb{F} of real or complex numbers, for vectors $u, v \in \mathbb{F}^N$, we denote its inner product as $\langle u, v \rangle = u^\dagger v$, where u^\dagger is the adjoint of u . For quantum states, we use the Dirac notation for inner product representation. We denote a vector's ℓ_2 norm by $\|v\| := \sqrt{\sum_{i=1}^N |v_i|^2} = \langle v, v \rangle$.

Let $\mathcal{M}_N(\mathbb{F})$ indicate the space of square matrices of size N on the field \mathbb{F} . For a matrix $A \in \mathcal{M}_N(\mathbb{C})$, let A_{ij} be the (i, j) -element of A . We denote the spectral norm by $\|A\| := \sup_{x \neq 0} \frac{\|Ax\|}{\|x\|} = \max_i \sigma_i(A)$, and the Frobenius norm by $\|A\|_F = \sqrt{\sum_i \sum_j |A_{ij}|^2} = \sqrt{\sum_{i=1}^N \sigma_i^2(A)}$, where $\sigma_i(A)$ are the singular values of A . We denote the transpose of A by A^\top , the adjoint of A by A^\dagger , and the pseudoinverse by A^{-1} . Note that $\|A^{-1}\| = \frac{1}{\sigma_{\min}(A)}$, where $\sigma_{\min}(A)$ is the smallest non-zero singular value of A . The condition number of A is denoted by $\kappa_A := \|A\| \|A^{-1}\| = \frac{\sigma_{\max}(A)}{\sigma_{\min}(A)}$. Finally, we denote the eigenvalues of A by $\lambda(A)$.

Lastly, we note that quantum circuits in this paper are ordered in the big endian format where the least significant qubit is placed as the bottom of the circuit.

Circulant matrices. In this paper, we discuss a special yet useful case of solving $Cx = b$, namely when C is a banded circulant matrix. We first lay the groundwork for our discussion with a set of definitions and properties of circulant matrices. A more in-depth review of such matrices can be referred to in [14, 25, 26].

Definition 1 (Circulant matrix). *Let $\mathbb{F} = \mathbb{R}$ or \mathbb{C} . A matrix $C \in \mathcal{M}_N(\mathbb{F})$ is called a circulant matrix if it takes the form*

$$C = \begin{pmatrix} c_0 & c_{N-1} & c_{N-2} & \cdots & c_1 \\ c_1 & c_0 & c_{N-1} & \cdots & c_2 \\ c_2 & c_1 & c_0 & \cdots & c_3 \\ \vdots & \vdots & \vdots & \ddots & \vdots \\ c_{N-1} & c_{N-2} & c_{N-3} & \cdots & c_0 \end{pmatrix}.$$

In this matrix, each column (row) vector is the previous column (row) cyclically shifted by one element. Given $\ell \in [N]$, any circulant matrix C can be written as a linear combination of *cyclic permutation matrices* $Q^\ell \in \mathcal{M}_N(\mathbb{R})$. That is,

$$C = \sum_{\ell=0}^{N-1} c_\ell Q^\ell, \quad Q = \begin{pmatrix} 0 & 0 & 0 & \cdots & 0 & 1 \\ 1 & 0 & 0 & \cdots & 0 & 0 \\ 0 & 1 & 0 & \cdots & 0 & 0 \\ \vdots & \vdots & \vdots & \ddots & \vdots & \vdots \\ 0 & 0 & 0 & \cdots & 1 & 0 \end{pmatrix}, \quad (1)$$

¹ Code implementation can be found at <https://github.com/LiXiufan/qa-cqs-circulant>.

One can see that C is normal and unitarily diagonalizable. The k -th eigenvalue of Q is given by $\lambda_k(Q) = \omega_N^k$, for all $k \in [N]$, where we have adopted the notation $\omega_N^k := e^{2\pi i k/N}$. The k -th eigenvalue of circulant matrix C is thus $\lambda_k(C) = \sum_{\ell=0}^{N-1} c_\ell \omega_N^{k\ell}$ for all $k \in [N]$. One can observe that the k -th eigenvector of C is $x^{(k)} = \frac{1}{\sqrt{N}} \left(1 \ \omega_N^k \ \omega_N^{2k} \ \dots \ \omega_N^{(N-1)k} \right)^\top$. Putting them together to form the diagonalizing matrix F , we see that $F_{jk} = \frac{1}{\sqrt{N}} \omega_N^{jk} = \frac{1}{\sqrt{N}} e^{2\pi i jk/N}$, or more explicitly,

$$F = \frac{1}{\sqrt{N}} \begin{pmatrix} & & & & & & \\ & & & & & & \\ & & & & & & \\ \dots & & \omega_N^{jk} & & & & \\ & & & & & & \\ & & & & & & \\ & & & & & & \end{pmatrix}. \quad (2)$$

This is the matrix form of the discrete Fourier transform (DFT), which can be used to diagonalize circulant matrices.

Banded circulant matrices. We now define the banded circulant matrix we aim to address in our paper.

Definition 2 (K -banded circulant matrix [26]). *Given $K \in \mathcal{O}(\text{poly log } N)$, a K -banded circulant matrix is a sparse circulant matrix where $c_{K+1}, c_{K+2}, \dots, c_{N-K-1} = 0$:*

$$C = \begin{pmatrix} c_0 & c_{N-1} & \dots & c_{N-K} & & c_K & \dots & c_1 \\ c_1 & c_0 & \dots & & & & & \vdots \\ \vdots & \dots & \dots & & & & & c_K \\ c_K & & \dots & \dots & \dots & \dots & & \\ & \dots & & \dots & \dots & \dots & & \\ & & \dots & & \dots & \dots & & c_{N-K} \\ c_{N-K} & & & \dots & \dots & \dots & & \vdots \\ \vdots & \dots & & & \dots & \dots & c_0 & c_{N-1} \\ c_{N-1} & \dots & c_{N-K} & & & c_K & \dots & c_1 & c_0 \end{pmatrix}$$

Noting that $Q^{N-\ell} = Q^{-\ell}$, we define $c_{-\ell} := c_{N-\ell}$ for $\ell \in [N]$. Therefore a K -banded circulant matrix can be expressed as a degree- $2K + 1$ matrix polynomial:

$$C = \sum_{\ell=-K}^K c_\ell Q^\ell. \quad (3)$$

III. SOLVING BANDED CIRCULANT LINEAR SYSTEMS

Problem statement. Let us be given a K -banded circulant matrix $C \in \mathcal{M}_N(\mathbb{C})$ and a normalized vector $\mathbf{b} \in \mathbb{C}^N$. Our task is to find a good estimator \tilde{x} for the least squares solution $x^* = C^{-1}\mathbf{b}$, such that the mean-square-error (MSE) loss of \tilde{x} , or $\|C\tilde{x} - \mathbf{b}\|^2$, is close to the MSE loss of x^* , or $\|Cx^* - \mathbf{b}\|^2$. More precisely, given additive error tolerance ε , we aim to find \tilde{x} such that

$$\mathcal{L}_{\text{MSE}}(\tilde{x}) := \|C\tilde{x} - \mathbf{b}\|^2 \leq \|Cx^* - \mathbf{b}\|^2 + \varepsilon = \min_{x \in \mathbb{C}^N} \|Cx - \mathbf{b}\|^2 + \varepsilon = \min_{x \in \mathbb{C}^N} \mathcal{L}_{\text{MSE}}(x) + \varepsilon. \quad (4)$$

High-level intuition. We follow the ideas introduced in [7] and divide the above problem into two parts. First, suppose we are given an Ansatz set of normalized vectors $\{\mathbf{u}_m\}_{m=1}^M$, where $\mathbf{u}_m \in \mathbb{C}^N$, such that estimator \tilde{x} can be constructed by finding a weighted combination of the Ansatz set where

$$\tilde{x}(\alpha) = \sum_{m=1}^M \alpha_m \mathbf{u}_m. \quad (5)$$

We then define the following problem:

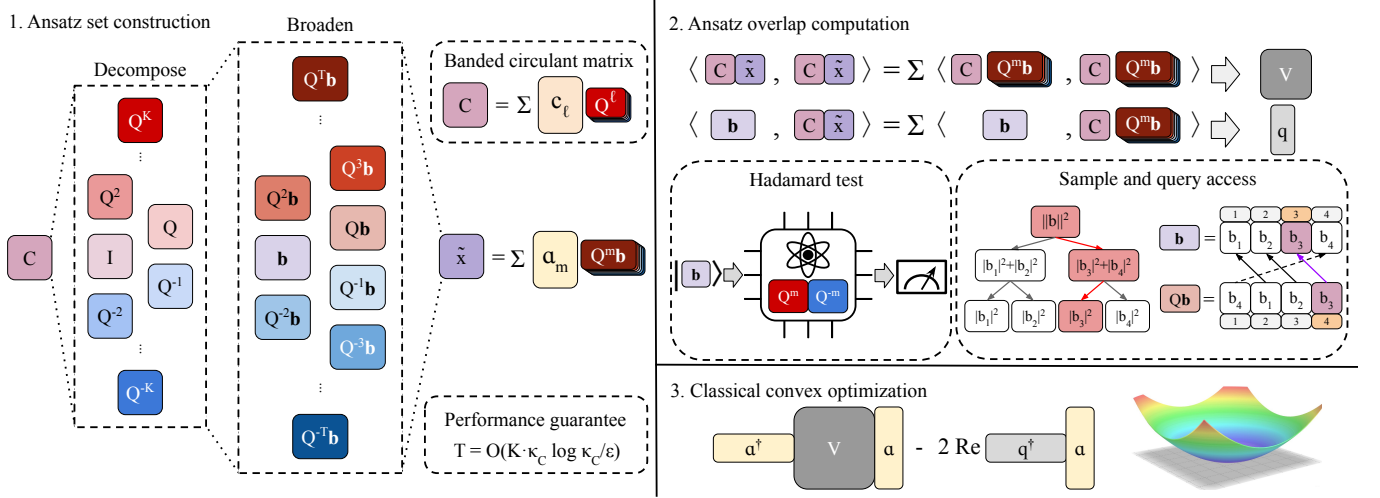


FIG. 1. Here we provide an illustrated overview of our method to solve K -banded circulant linear systems. Note the fact that C can be written as a matrix polynomial in terms of the cyclic permutation matrix Q given in Equation 1 with the powers being bounded between $-K$ and K . In step (1), we set a truncation threshold $T \geq K$ to create a matrix polynomial with powers of Q from $-T$ to T that serves as an approximation to C^{-1} . To find the optimal coefficients of the matrix polynomial α , in step (2), we calculate the overlaps between individual components $CQ^m \mathbf{b}$ as well as the overlap between $CQ^m \mathbf{b}$ and \mathbf{b} . Such overlaps can be computed with either the Hadamard test for the hybrid quantum-classical algorithm or sample and query access for the quantum-inspired algorithm. Lastly, in step (3) we perform classical convex optimization to find the optimal coefficients α .

Definition 3 (CIRCULANTOPTIM). *We are given a K -banded circulant matrix $C \in \mathcal{M}_N(\mathbb{C})$ with the decomposition $C = \sum_{\ell=-K}^K c_\ell Q^\ell$, where $K \in \mathcal{O}(\text{poly log } N)$, as well as a vector $\mathbf{b} \in \mathbb{C}^N$. An Ansatz set $\{\mathbf{u}_m\}_{m=1}^M$, and error tolerance $\zeta > 0$ are also provided. The problem is to find $\{\hat{\alpha}_m\}_{m=1}^M$, $\alpha_m \in \mathbb{C}$ such that*

$$\left\| C \sum_{m=1}^M \hat{\alpha}_m \mathbf{u}_m - \mathbf{b} \right\|^2 \leq \min_{\alpha \in \mathbb{C}^M} \left\| C \sum_{m=1}^M \alpha_m \mathbf{u}_m - \mathbf{b} \right\|^2 + \zeta.$$

By expanding the MSE loss term, we see that the above problem can be solved by convex optimization methods given that bounded error approximations of inner products of $\langle C\mathbf{u}_k, C\mathbf{u}_m \rangle$ and $\langle \mathbf{b}, C\mathbf{u}_m \rangle$ are computed. This serves as the bottleneck to this problem as the computation of inner products may scale linearly with the dimension of the vector, a costly operation when dealing with high dimensional data. However, in different formulations of the problem where vector \mathbf{b} and the Ansatz set are given as quantum circuits or given with sample and query access, the problem variants may have a $\text{poly log } N$ algorithm. We discuss the implementations of these methods in Sections IV and V, while the hardness of the variant problems is discussed in Section VI.

Second, we have to provide a suitable Ansatz set $\{\mathbf{u}_m\}_{m=1}^M$ such that

$$\min_{\alpha \in \mathbb{C}^M} \left\| C \sum_{m=1}^M \alpha_m \mathbf{u}_m - \mathbf{b} \right\|^2 \leq \min_{x \in \mathbb{C}^N} \|Cx - \mathbf{b}\|^2 + \nu. \quad (6)$$

By setting $\zeta = \nu = \varepsilon/2$, we recover the requirement in Equation 4. As C can be expressed as a polynomial in terms of Q , to approximate C^{-1} one can simply explore the Krylov subspaces $\mathcal{K}(Q, \mathbf{b})$ and $\mathcal{K}(Q^{-1}, \mathbf{b})$ to obtain an approximation of $C^{-1}\mathbf{b}$ [7, 27, 28]. Hence, given a truncation threshold T for the exploration of the two Krylov subspaces, we can create an Ansatz set $\{\mathbf{u}_m = Q^m \mathbf{b}\}_{m=-T}^T$, the linear combination of which can then be used to approximate $C^{-1}\mathbf{b}$.

Algorithm. We employ the CQS technique by Huang *et al.* [7] and use Algorithm 1 to solve the given circulant linear system of equations. An overview can be found in Figure 1. We outline the idea behind the algorithm below.

Per high-level intuition, we see that the estimator \tilde{x} is assembled from a set of quantum states such that given truncation threshold $T \geq K$, we have the tunable parameter set $\alpha := \{\alpha_i : \alpha_i \in \mathbb{C}\}$ and

$$\tilde{x}(\alpha) = \sum_{m=-T}^T \alpha_m \mathbf{u}_m = \sum_{m=-T}^T \alpha_m Q^m \mathbf{b}. \quad (7)$$

Algorithm 1 High-level algorithm for solving banded circulant linear systems

Input: Decomposition coefficients of K -banded circulant matrix $\{c_\ell\}_{\ell \in [-K..K]}$, Normalized column vector \mathbf{b} , Truncation threshold T .

Output: Combination parameters $\{\alpha_m\}_{m \in [-T..T]}$, Sketches of $\{\mathbf{u}_m : \mathbf{u}_m = Q^m \mathbf{b}, \forall m \in [-T..T]\}$

- 1: Estimate entry values of matrix $V^R \in \mathcal{M}_{2T+1}(\mathbb{R})$, where $V_{jk}^R = \text{Re} \left(\sum_{y=-K}^K \sum_{z=-K}^K c_y^* c_z \langle \mathbf{b}, Q^{y-z+k-j} \mathbf{b} \rangle \right)$.
 - 2: Estimate entry values of matrix $V^I \in \mathcal{M}_{2T+1}(\mathbb{R})$, where $V_{jk}^I = \text{Im} \left(\sum_{y=-K}^K \sum_{z=-K}^K c_y^* c_z \langle \mathbf{b}, Q^{y-z+k-j} \mathbf{b} \rangle \right)$.
 - 3: Estimate entry values of vector $q^R \in \mathbb{R}^{2T+1}$, where $q_j^R = \text{Re} \left(\sum_{y=-K}^K c_y \langle \mathbf{b}, Q^{y+j} \mathbf{b} \rangle \right)$.
 - 4: Estimate entry values of vector $q^I \in \mathbb{R}^{2T+1}$, where $q_j^I = \text{Im} \left(\sum_{y=-K}^K c_y \langle \mathbf{b}, Q^{y+j} \mathbf{b} \rangle \right)$.
 - 5: Let $W = \begin{pmatrix} V^R & -V^I \\ V^I & V^R \end{pmatrix}$ and $r = \begin{pmatrix} q^R \\ q^I \end{pmatrix}$.
 - 6: Solve for z in convex optimization problem $z^\top W z - 2r^\top z + 1$.
 - 7: $\forall m \in [-T..T]$, let $\alpha_m = z_m + i \cdot z_{2T+1+m}$.
 - 8: **return** $\{(\alpha_m, Q^m \mathbf{b})\}_{m \in [-T..T]}$
-

We minimize the combination parameters α over the MSE loss

$$\mathcal{L}_{\text{MSE}}(\tilde{x}) = \|C\tilde{x} - \mathbf{b}\|^2 = \langle C\tilde{x}, C\tilde{x} \rangle - 2 \text{Re}\{\langle \mathbf{b}, C\tilde{x} \rangle\} + 1, \quad (8)$$

to achieve an approximation to x^* . Following [7], we construct the complex matrix $V \in \mathcal{M}_{2T+1}(\mathbb{C})$ and complex vector $q \in \mathbb{C}^{2T+1}$ with $V_{jk} := \langle C\mathbf{u}_j, C\mathbf{u}_k \rangle$ and $q_j := \langle \mathbf{b}, C\mathbf{u}_j \rangle$ such that

$$\|C\tilde{x} - \mathbf{b}\|^2 = \alpha^\dagger V \alpha - 2 \text{Re}\{q^\dagger \alpha\} + 1. \quad (9)$$

We note that the terms V_{jk} and q_j can be computed from the summation of inner products of the form $\langle \mathbf{b}, Q^j \mathbf{b} \rangle$ for $k \in [-2T - 2K..2T + 2K]$:

$$V_{jk} = \langle C\mathbf{u}_j, C\mathbf{u}_k \rangle = \sum_{y=-K}^K \sum_{z=-K}^K c_z^* c_y \langle \mathbf{b}, Q^{y-z+k-j} \mathbf{b} \rangle, \quad (10)$$

$$q_j = \langle \mathbf{b}, C\mathbf{u}_j \rangle = \sum_{y=-K}^K c_y \langle \mathbf{b}, Q^{y+j} \mathbf{b} \rangle. \quad (11)$$

To solve for the combination parameters α , we define the auxiliary system matrix $W \in \mathcal{M}_{4T+2}(\mathbb{R})$ and vector $r \in \mathbb{R}^{4T+2}$:

$$W := \begin{pmatrix} \text{Re}\{V\} & -\text{Im}\{V\} \\ \text{Im}\{V\} & \text{Re}\{V\} \end{pmatrix}, \quad r := \begin{pmatrix} \text{Re}\{q\} \\ \text{Im}\{q\} \end{pmatrix}. \quad (12)$$

We can then recast the above problem into a convex optimization problem involving a real vector $z \in \mathbb{R}^{4T+2}$ with $z := (\text{Re}\{\alpha\}, \text{Im}\{\alpha\})^\top$. The problem becomes

$$\min_{z \in \mathbb{R}^{4T+2}} z^\top W z - 2r^\top z + 1. \quad (13)$$

Solving for z gives us the real and imaginary parts of all coefficients in the set $\{\alpha_m\}_{m=-T}^T$. Recalling that our goal is to obtain an estimator \tilde{x} of x^* , we can represent \tilde{x} by combining the coefficients α and classical sketches of the vectors $\{\mathbf{u}_m = Q^m \mathbf{b}\}_{m=-T}^T$. Note that we do not obtain the explicit value of \tilde{x} . We will address such limitations at the end of this section.

Performance guarantee. We provide a provable guarantee for the selection of truncation threshold T such that $\mathcal{L}_{\text{MSE}}(\tilde{x})$ is ν -close to $\min_{x \in \mathbb{C}^N} \mathcal{L}_{\text{MSE}}(x)$. The proof can be found in Appendix A.

Proposition 4. *Let $0 < \nu \leq 1$. Given a K -banded circulant matrix $C \in \mathcal{M}_N(\mathbb{C})$ where $\kappa_C = \|C\| \|C^{-1}\|$ and a normalized vector $\mathbf{b} \in \mathbb{C}^N$, there exists $T \in \mathcal{O}(K \cdot \kappa_C \log \frac{\kappa_C}{\nu})$ such that we can find an optimal set of parameters $\alpha = \{\alpha_m \in \mathbb{C}, \forall m \in [-T..T]\}$ and that the estimator $\tilde{x}(\alpha) = \sum_{m=-T}^T \alpha_m Q^m \mathbf{b}$ satisfies*

$$\min_{\alpha \in \mathbb{C}^{2T+1}} \|C\tilde{x}(\alpha) - \mathbf{b}\|^2 \leq \min_{x \in \mathbb{C}^N} \|Cx - \mathbf{b}\|^2 + \nu.$$

We note that the above proposition provides a tighter bound on the number of quantum states required compared to the $(2K+1)^{\mathcal{O}(\kappa_C \log \frac{\kappa_C}{\nu})}$ upper bound of a full Ansatz tree obtained by Huang *et al.* [7]. In addition, our solution only requires solving the convex optimization problem once, as opposed to the iterative solution with the original CQS with the gradient expansion approach to Ansatz trees. Further, our results also suggest that the CQS strategy can be applied directly to non-Hermitian banded circulant matrices C without having to transform the matrix into a Hermitian one via embedding tricks.

Limitations. As mentioned, Algorithm 1 provides \tilde{x} as a weighted combination of vectors that exist in the direct sum of the Krylov subspaces $\mathcal{K}_T(Q, \mathbf{b})$ and $\mathcal{K}_T(Q^{-1}, \mathbf{b})$ instead of an explicit vector. Such representations are useful for investigating certain properties of x , such as the expectation $x^\dagger M x$ for some operator M , but the actual vector cannot be retrieved without an exponential-cost post-processing procedure. Such limitations have also been found [29] in the HHL algorithm [1], which produces the solution as a quantum state $|x\rangle$, with the retrieval of the explicit vector x requiring exponential cost as well.

For the output of Algorithm 1, note that we output both the coefficients $\{\alpha_m\}_{m=-T}^T$ and sketches of the corresponding Ansatz set $\{\mathbf{u}_m\}$ to form a representation of \tilde{x} . For the quantum algorithm, quantum circuits that prepare $|u_m\rangle$ are prepared, while for the quantum-inspired algorithm, data structures that provide sample and query access to vectors \mathbf{u}_m are provided. We detail the preparation of these sketches in Sections IV and V respectively.

Finally, Proposition 4 guarantees that the loss of the solution that Algorithm 1 provides will converge if the truncation threshold $T \in \mathcal{O}(K \cdot \kappa_C \log \kappa_C / \epsilon)$. This means that for ill-conditioned banded circulant matrices where $\kappa_C \rightarrow \infty$, we do not provide an effective guarantee of convergence, which also occurs in classical Krylov subspace-based algorithms such as the conjugate gradient method [16]. However, this does not mean that the algorithm will not converge; Proposition 4 only provides an upper bound for convergence guarantees. Convergence may still occur with truncation thresholds lower than the upper bound limit, a trait observed in our numerical results in Section VII.

IV. HYBRID ALGORITHM AND QUANTUM CIRCUIT IMPLEMENTATION

We now elaborate on the implementation of Algorithm 1 using quantum hardware. Without loss of generality, let $n = \lceil \log_2 N \rceil$. Given an n -qubit quantum system, to implement the algorithm, we require the following assumption:

Assumption 5. *Assume that there exists a hardware-efficient n -qubit quantum circuit evaluating unitary U_b such that normalized vector \mathbf{b} can be implemented as a quantum state $|\mathbf{b}\rangle = U_b |0^n\rangle$ with $\mathcal{O}(\text{poly } n)$ circuit depth.*

We implement steps 1-4 of Algorithm 1 with quantum computers, obtaining estimations of each entry of V^R , V^I , q^R , and q^I with the Hadamard test [22], which are then stored in classical memory. We modify quantum circuit implementations of shift operations shown by Koch *et al.* [30] and quantum adder circuit by Draper [31] to implement the cyclic permutation operator Q and its powers with circuit depth independent to the power m , a contrast to the implementation of quantum circuits for solving general linear systems by Huang *et al.* [7]. Steps 5-8 of the algorithm remain implemented on classical computers. As shown in the following section, the powers of Q can be implemented with a known quantum circuit with $\mathcal{O}(n^2)$ quantum gates. Therefore, we can construct classical sketches of the circuit implementation of output states $|u_m\rangle = Q^m U_b |0^n\rangle$ that correspond to the computed optimal parameters α_m , using $\mathcal{O}(Tn^2)$ memory in total to provide a classical sketch of the estimator \tilde{x} as a combination of quantum states. We now provide details of the circuit implementation as follows:

Quantum circuit implementation. Recall from Section II that the eigendecomposition of the cyclic permutation matrix Q is given by $Q = F^{-1} \Lambda F$, where Λ is the diagonal matrix with all eigenvalues of Q and the diagonalization matrix F is the matrix representation of DFT. On quantum systems, for cases where $n = \log_2(N)$, F can be implemented with $\mathcal{O}(n^2)$ quantum logic gates using the quantum Fourier transform (QFT) [17]. For the more general case where $n \neq \log_2 N$, one can use the arbitrary-size quantum Fourier transform proposed by Kitaev [32] which utilizes quantum phase estimation to construct DFT. As such implementations require fault-tolerance, we discuss only the standard QFT for our implementation, while details on the generalized case are provided in Appendix B.

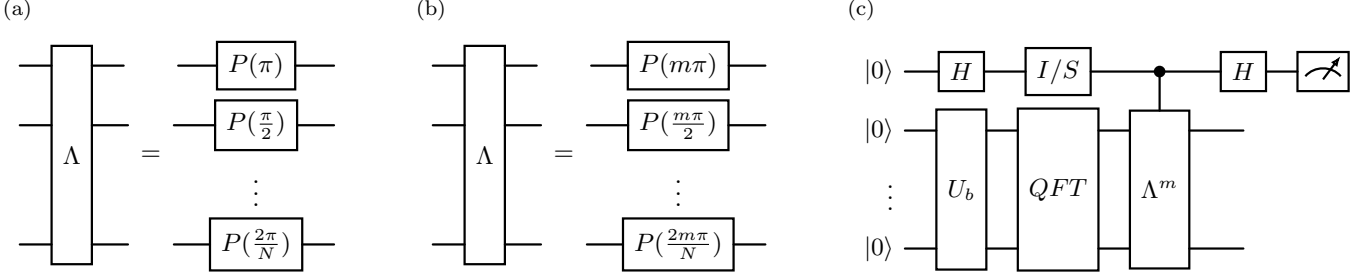


FIG. 2. Circuit implementation of quantum subroutines in our algorithm. The cyclic permutation matrix Q can be diagonalized by the DFT matrix F such that $Q = F^{-1}\Lambda F$. DFT can be implemented by QFT circuits. See Appendix B for the implementation of QFT for arbitrary N . The diagonal matrix Λ can be implemented as a tensor product of phase gates as shown in Panel 2a. Powers of Λ can be implemented with the same phase gates, by multiplied rotation angles as shown in Panel 2b. To retrieve the real and imaginary parts of $\langle b|Q^m|b\rangle$, we use the Hadamard test (on the state $QFT|b\rangle$), which requires a controlled version of Λ^m , i.e. controlled phase gates, as shown in Panel 2c.

For the remainder of the discussion, we assume $n = \log_2(N)$, while keeping in mind that cases where $n \neq \log_2(N)$ are still implementable. Matrix Λ can be written as:

$$\Lambda = \text{diag}(\omega_N^0 \ \omega_N^1 \ \omega_N^2 \ \cdots \ \omega_N^{N-1}) \quad (14)$$

We use the phase gate P , whose matrix form is

$$P(\theta) = \begin{pmatrix} 1 & 0 \\ 0 & e^{i\theta} \end{pmatrix}, \quad (15)$$

where the parameter θ is the rotation angle. We note that $\omega^0 = 1$. Hence Λ can be written as the tensor product of $P(\theta)$ gates as follows:

$$\Lambda = \begin{pmatrix} 1 & 0 \\ 0 & \omega_{N/2}^1 \end{pmatrix} \otimes \cdots \otimes \begin{pmatrix} 1 & 0 \\ 0 & \omega_N^1 \end{pmatrix} \otimes \begin{pmatrix} 1 & 0 \\ 0 & \omega_N^0 \end{pmatrix} = \bigotimes_{j=0}^{n-1} P(\theta_j), \quad \text{where } \theta_j = \frac{2\pi}{N} \cdot 2^j. \quad (16)$$

The implementation of Λ is then as illustrated in Figure 2a. We note that this is the non-controlled version of the quantum adder circuit proposed by Draper [31]. The number of gates for this implementation is equal to the qubit number n .

We note that for $m \in \mathbb{Z}$, Q^m has eigendecomposition $F^{-1}\Lambda^m F$. Further note that the powers of phase operations are phase operations with multiplied rotation angles, that is, $P(\theta)^m = P(m\theta)$. As Λ can be decomposed into a tensor product of phase gates, we can simply implement Λ^m with the same gate, but with the angles multiplied by m , as shown in Figure 2b. Observe that the implemented quantum circuit is independent of m and only depends on the depth of the QFT implementation.

Given the above implementation of powers of Q , to obtain the expectation value of $\langle b|Q^m|b\rangle$, we prepare a quantum state $|\psi_b\rangle = QFT|b\rangle$. A Hadamard test is then performed on Λ^m to calculate the expectation values with respect to $|\psi_b\rangle$ as described in Appendix B, such that we obtain the values of $\text{Re}\langle\psi_b|\Lambda^m|\psi_b\rangle$ and $\text{Im}\langle\psi_b|\Lambda^m|\psi_b\rangle$, which are equivalent to $\text{Re}\langle b|Q^m|b\rangle$ and $\text{Im}\langle b|Q^m|b\rangle$. The full quantum circuit is shown in Figure 2c.

Number of total measurements. As we conduct quantum measurements to obtain auxiliary system matrices W and r , we do not gain the exact value of the entries in the matrices. Instead, what we obtain are estimations of the values whose accuracy depends on the number of measurements conducted. The total number of measurements required to achieve a close enough estimate of \tilde{x} is stated in the following proposition:

Proposition 6 (Number of measurements needed). *Given K -banded circulant matrix $C = \sum_{\ell=-K}^K c_\ell Q^\ell \in \mathcal{M}_N(\mathbb{C})$, hardware efficient implementation of U_b as shown in Assumption 5 and truncation threshold T . This defines auxiliary systems W and r in Equation 12. Let the sum of absolute values of the coefficients of decomposed C be $B = \sum_{\ell=-K}^K |c_\ell|$. We can find $\tilde{\alpha} : \{\tilde{\alpha}_m \in \mathbb{C}, \forall m \in [-T..T]\}$ for estimator $\tilde{x}(\alpha) = \sum_{m=-T}^T \alpha_m Q^m U_b |0^n\rangle$ such that the following is satisfied*

$$\|C\tilde{x}(\tilde{\alpha}) - |b\rangle\|^2 \leq \min_{\alpha \in \mathbb{C}^{2T+1}} \|C\tilde{x}(\alpha) - |b\rangle\|^2 + \varepsilon$$

using $\mathcal{O}(B^4(K+T)T\|W\|\|W^{-1}\|^2(1+\|W^{-1}r\|^2/\varepsilon))$ measurements via Hadamard test.

Algorithm 2 Classical subroutine for inner product estimation with sample and query access

Input: Classical data structure \mathcal{S}_b as shown in Assumption 8, Power of cyclic perturbation matrix m , Additive error ε , Failure rate δ

Output: ε -close estimation of $\langle \mathbf{b}, Q^m \mathbf{b} \rangle$ with success rate $1 - \delta$

```

1: for  $i \leftarrow 0$  to  $6 \log(2/\delta)$  do
2:    $\eta_i \leftarrow 0$ 
3:   for  $j \leftarrow 0$  to  $9/\varepsilon^2$  do
4:      $s \leftarrow \text{SAMPLE}(\mathcal{S}_b)$ 
5:      $q \leftarrow \text{QUERY}(\mathcal{S}_b, s - m \pmod{N})$ 
6:      $r \leftarrow \text{QUERY}(\mathcal{S}_b, s)$ 
7:      $\eta_i \leftarrow \eta_i + q/r$ 
8:   end for
9:    $\eta_i \leftarrow \eta_i \varepsilon^2 / 9$ 
10: end for
11: return MEDIAN( $\eta$ )

```

We note that the number of different expectation values needed is $4K + 4T + 1 \in \mathcal{O}(K + T)$ due to the high overlap of values required. So the number of total measurements for all entries on W and r to have variance $\mathcal{O}(1/R)$ is $\mathcal{O}((K + T)B^4R)$. From Proposition 12 of [7], we have $R > CT\|W\|\|W^{-1}\|^2(1 + \|W^{-1}r\|^2/\varepsilon)$.

We now provide informal bounds of the above proposition. Based on discussions given by Huang *et al.* [7] on the upper bounds of $\|W\|$, $\|W^{-1}\|$ and $\|W^{-1}r\|$, we can see that the number of measurements in the proposition can be expressed as

$$\mathcal{O}\left(\frac{(K + T)TB^4\kappa_C^2}{\varepsilon^5}\right). \quad (17)$$

Further, in order to achieve an ε -close solution to the optimal x^* where $x^* = \operatorname{argmin}_{x \in \mathbb{C}^N} \|Cx - b\|^2$, we note by Proposition 4 that $T \in \mathcal{O}(K \cdot \kappa_C \log \frac{\kappa_C}{\varepsilon})$. Hence the total number of measurements needed is

$$\mathcal{O}\left(\frac{K^2B^4\kappa_C^4}{\varepsilon^5} \log \frac{\kappa_C}{\varepsilon}\right). \quad (18)$$

V. QUANTUM-INSPIRED ALGORITHM

We now elaborate on the implementation of Algorithm 1 using purely classical computers that achieve the same performance as the hybrid implementation. To do so, we simply replace the Hadamard test subroutine with a classical subroutine that utilizes techniques used by Tang [8] to estimate inner products. To use these techniques, we require sample and query access to the vector \mathbf{b} .

Definition 7 (Sample and query access [8, 33]). *For vector $x \in \mathbb{C}^N$, let \mathcal{D}_x be the distribution over $[N]$ such that a sample $X \sim \mathcal{D}_x$ satisfies $\Pr(X = k) = \frac{|x_k|^2}{\|x\|_2^2}$. A sample access of x returns $k \in [N]$ over \mathcal{D}_x . A query access of x with supplied index k returns the k -th element of x .*

We then make the following assumption:

Assumption 8. *Assume that there exists a classical data structure \mathcal{S}_b containing sufficient information of vector \mathbf{b} such that command $\text{SAMPLE}(\mathcal{S}_b)$ achieves sample access to \mathbf{b} and command $\text{QUERY}(\mathcal{S}_b, i)$ achieves query access to the i -th element of \mathbf{b} . Further, assume that the input of vector \mathbf{b} to Algorithm 1 is given in the form of \mathcal{S}_b .*

A binary tree implementation of such a data structure has been shown by Chia *et al.* [9]. The leaf nodes of the tree stores the square of the absolute value of each entry, in addition to its original value, while the internal nodes store the sum of their children. As a result, the root node stores the square of the ℓ_2 norm of the vector. Each sample and query access then requires $\mathcal{O}(\log N)$ time.

Although the hybrid algorithm partially implemented on quantum hardware decomposes Q into a QFT operation and phase shift operations, the quantum-inspired version does not perform any Fourier-related operations due to its high classical time complexity. Instead, we use the fact that the application of Q on vector \mathbf{b} performs a cyclic

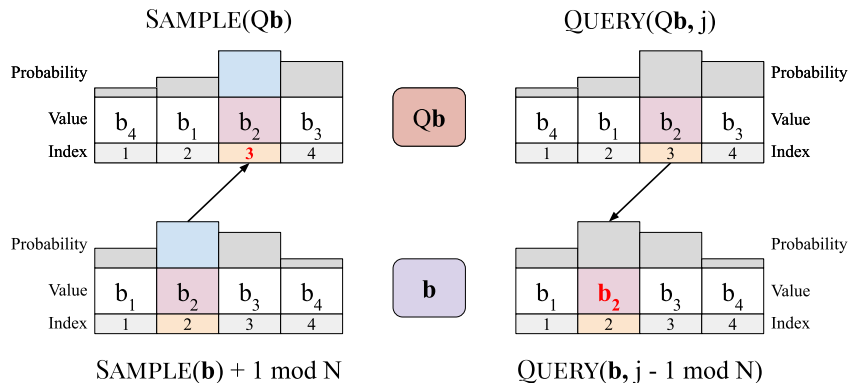


FIG. 3. We illustrate how sample and query access to vector \mathbf{b} provides the same access to \mathbf{Qb} . Sample access to \mathbf{Qb} is equivalent to shifting the output of sample access to \mathbf{b} , while query access to \mathbf{Qb} is equivalent to shifting the input to query access to \mathbf{b} . Note that sample access to \mathbf{Qb} is not needed for Algorithm 2.

permutation of vector \mathbf{b} . Observe that the query access to $Q^m \mathbf{b}$ retrieves the elements of b shifted m times to the right and sample access to $Q^m \mathbf{b}$ outputs an index that corresponds to the index m times to the right of the original vector \mathbf{b} , as illustrated in Figure 3.

We estimate the value of $\langle \mathbf{b}, Q^m \mathbf{b} \rangle$ by Algorithm 2, which is modified from Algorithm 1 of [33], and whose performance guarantee of requiring $\mathcal{O}(\frac{1}{\varepsilon^2} \log \frac{1}{\delta})$ sample and query accesses to execute is ensured by Proposition 3 of the same paper. Such a process can effectively replace the use of Hadamard tests, allowing us to perform Steps 1 to 4 of Algorithm 1 on classical computers.

Further, the classical sketch of the output vectors \mathbf{u}_m can be constructed by using an index shifting wrapper function \mathcal{F}_m that wraps data structure $\mathcal{S}_{\mathbf{b}}$ such that the command $\text{SAMPLE}(\mathcal{F}_m(\mathcal{S}_{\mathbf{b}}))$ returns $\text{SAMPLE}(\mathcal{S}_{\mathbf{b}}) + m \pmod{N}$ and command $\text{QUERY}(\mathcal{F}_m(\mathcal{S}_{\mathbf{b}}, i))$ returns $\text{QUERY}(\mathcal{S}_{\mathbf{b}}, i - m \pmod{N})$. We can see that the sample and query accesses to $\mathcal{S}_{\mathbf{u}_m}$ is equivalent to $\mathcal{F}_m(\mathcal{S}_{\mathbf{b}})$, and $\mathcal{F}_m(\mathcal{S}_{\mathbf{b}})$ can be used to represent the sketch for $\mathcal{S}(\mathbf{u}_m)$.

With the above, we have produced a quantum-inspired classical algorithm with the same performance guarantee. Note that the total number of query and sample accesses required to execute Algorithm 1 matches the upper bound of quantum measurements required as supplied in Proposition 6, which we restate in the current setting:

Lemma 9 (Number of sample/query accesses needed). *Given K -banded circulant matrix $C = \sum_{\ell=-K}^K c_{\ell} Q^{\ell} \in \mathcal{M}_N(\mathbb{C})$, classical data structure $\mathcal{S}_{\mathbf{b}}$ as shown in Assumption 8 and truncation threshold T . This defines the auxiliary systems W and r in Equation 12. Let the sum of absolute values of the coefficients of decomposed C be $B = \sum_{\ell=-K}^K |c_{\ell}|$. We can find $\tilde{\alpha} : \{\tilde{\alpha}_m \in \mathbb{C}, \forall m \in [-T..T]\}$ for estimator $\tilde{x}(\alpha) = \sum_{m=-T}^T \alpha_m Q^m \mathbf{b}$ such that the following is satisfied*

$$\|C\tilde{x}(\tilde{\alpha}) - \mathbf{b}\| \leq \min_{\alpha \in \mathbb{C}^{2t+1}} \|C\tilde{x}(\alpha) - \mathbf{b}\| + \varepsilon$$

using $\mathcal{O}(B^4(K+T)T\|W\|\|W^{-1}\|^2(1+\|W^{-1}r\|^2/\varepsilon))$ sample and query accesses to $\mathcal{S}_{\mathbf{b}}$.

While Algorithm 2 can be dequantized with all quantum subroutines being discarded, we note that Assumption 8 is rather strong, and the preparation of $\mathcal{S}_{\mathbf{b}}$ may take up to $\mathcal{O}(N)$ time. Similarly, there is no guarantee that $|b\rangle$ can be effectively prepared on a quantum computer, hence the bottleneck of such algorithms lies in the preparation of the vector \mathbf{b} for our algorithms, rather than the algorithms themselves.

VI. COMPLEXITY AND HARDNESS

As convex optimization is performed classically and the inner product estimation subroutine can be implemented classically, a natural question that arises is whether the hybrid algorithm provides value. In this section, we discuss this problem by analyzing the complexity and hardness of two variants of the CIRCULANTOPTIM problem as seen in Definition 3, QUANTUMCIRCULANTOPTIM and SAMPLECIRCULANTOPTIM, which correspond to solving for the coefficients α after all the inner products required in Algorithm 1 are evaluated by Hadamard tests for quantum computers or Algorithm 2 for classical computers. Note that the hybrid algorithm and the quantum-inspired algorithm solve different problems due to their distinctively different settings of the input vector. Therefore, our discussion below does not imply any relationship between the complexity classes PromiseBQP and PromiseBPP.

We first discuss the hybrid algorithm case. Suppose there are efficient quantum circuits that prepare \mathbf{b} and all vectors in $\{\mathbf{u}_m\}_{m=1}^M$, we can define the following problem:

Definition 10 (QUANTUMCIRCULANTOPTIM). *We are given a K -banded circulant matrix $C \in \mathcal{M}_N(\mathbb{C})$ which has the decomposition $C = \sum_{\ell=-K}^K c_\ell Q^\ell$, where $K \in \mathcal{O}(\text{poly log } N)$, as well a quantum circuit with oracle access with depth $\mathcal{O}(\text{poly log } N)$ that can generate given $\mathbf{b} \in \mathbb{C}^N$ as a $\log N$ -qubit quantum state $|b\rangle$. Quantum circuits that generate the Ansatz set of $\log N$ -qubit quantum states $\{|u_m\rangle\}_{m=1}^M$, and error $\zeta > 0$ are also provided. The problem is to find $\{\hat{\alpha}_m\}_{m=1}^M, \alpha_m \in \mathbb{C}$ such that*

$$\left\| C \sum_{m=1}^M \hat{\alpha}_m |u_m\rangle - |b\rangle \right\|^2 \leq \min_{\alpha \in \mathbb{C}^M} \left\| C \sum_{m=1}^M \alpha_m |u_m\rangle - |b\rangle \right\|^2 + \zeta.$$

Note that the problem here is not merely a subproblem of the coefficient optimization problem in the $Ax = b$ linear solver shown by Huang *et al.* [7], as we do not restrict C to be Hermitian. Furthermore, we have the following proposition, whose proof is provided in Appendix C.

Proposition 11. *If there exists a relativizing classical algorithm that solves QUANTUMCIRCULANTOPTIM in $\text{poly}(\kappa_C, \log N)$ time, then $\text{PromiseBQP} = \text{PromiseBPP}$.*

For the sample and query quantum-inspired classical algorithm, we define a similar problem.

Definition 12 (SAMPLECIRCULANTOPTIM). *We are given a K -banded circulant matrix $C \in \mathcal{M}_N(\mathbb{C})$ which has the decomposition $C = \sum_{\ell=-K}^K c_\ell Q^\ell$, where $K \in \mathcal{O}(\text{poly log } N)$, as well as sample and query access to $\mathbf{b} \in \mathbb{C}^N$. Query access to the Ansatz set $\{\mathbf{u}_m\}_{m=1}^M, \mathbf{u}_m \in \mathbb{C}^N$, and error $\zeta > 0$ are also provided. The problem is to find $\{\hat{\alpha}_m\}_{m=1}^M, \alpha_m \in \mathbb{C}$ such that*

$$\left\| C \sum_{m=1}^M \hat{\alpha}_m \mathbf{u}_m - \mathbf{b} \right\|^2 \leq \min_{\alpha \in \mathbb{C}^M} \left\| C \sum_{m=1}^M \alpha_m \mathbf{u}_m - \mathbf{b} \right\|^2 + \zeta.$$

We emphasize again that this result does not imply any relationship between PromiseBPP and PromiseBQP . Although QUANTUMCIRCULANTOPTIM and SAMPLECIRCULANTOPTIM are both variants of the CIRCULANTOPTIM, the input assumptions on \mathbf{b} and Ansatz set $\{\mathbf{u}_m\}_{m=1}^M$ in these two problems make them distinctively different. The conversion of the sample and query access data structure \mathcal{S}_b to a quantum state $|b\rangle$ requires N query access to reproduce the actual vector \mathbf{b} and encode it into a quantum state. Conversely, to produce \mathcal{S}_b , each individual element of vector representation has to be retrieved from the quantum state $|b\rangle$, which is converted to \mathcal{S}_b . As such conversions have an exponential cost, to our knowledge, one cannot reduce QUANTUMCIRCULANTOPTIM to SAMPLECIRCULANTOPTIM and vice versa unless $\text{PromiseBQP} = \text{PromiseBPP}$.

VII. APPLICATIONS AND NUMERICAL RESULTS

In this section, we consider the applications of solving banded circulant linear systems in finding solutions to partial differential equations (PDEs) with periodic boundaries. We consider the heat transfer problem in particular and obtain numerical results in solving the corresponding circulant linear systems.

One-dimensional heat transfer problem. Solving heat transfer problems with quantum methods has been previously researched by Guseynov *et al.* [34]. They tackle the problem by applying QFT and using the variational quantum linear solver (VQLS) [4] for optimization in the Fourier domain. In addition, they also propose a CQS-Ansatz tree-based approach which first converts the circulant matrix into the Fourier domain using QFT and then decomposes the Fourier representation into Pauli matrices. Their method requires gradient heuristics for potential speedups as the inclusion of all Pauli matrices in the Ansatz tree to provide theoretical guarantees results in an exponential number of terms in the qubit number. In comparison, we employ Algorithm 1 for circulant linear systems with either the Hadamard test shown in Figure 2c, which uses QFT as diagonalization, or, for the quantum-inspired algorithm, the subroutine shown in Algorithm 2, which does not incorporate DFT at all.

For simplicity, we consider only the one-dimensional heat transfer problem. We denote the spatial variable by $x \in \mathbb{R}$ and the thermal diffusivity by $a \in \mathbb{C}$. The heat conduction equation is then given by

$$a^2 \Delta \Phi(x, t) - \frac{\partial \Phi(x, t)}{\partial t} = f(x, t), \quad (19)$$

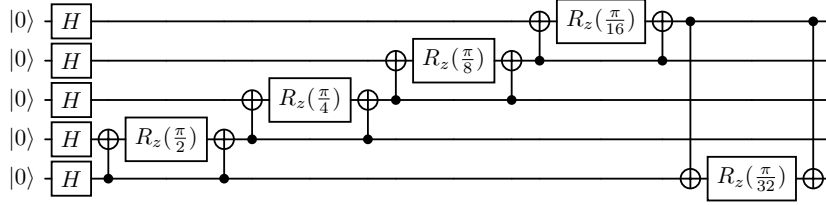


FIG. 4. State preparation circuit of $|b\rangle$ modeled after the QAOA circuit [35, 36].

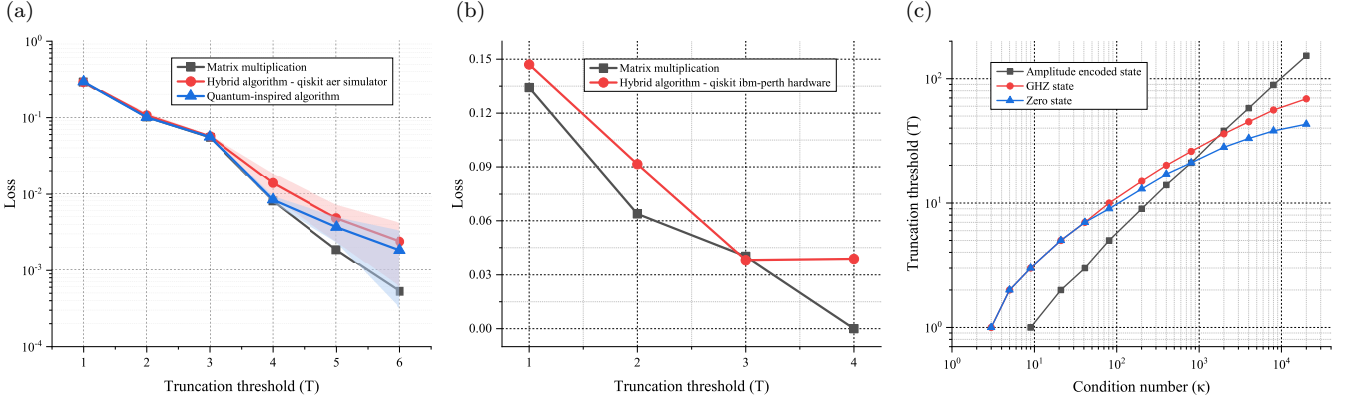


FIG. 5. Numerical results of hybrid and quantum-inspired algorithms proposed in our paper for solving heat conduction linear systems. First, we show that simulation results of our hybrid and quantum-inspired algorithms can provide decent approximations to the results obtained by matrix multiplication in Panel 5a, with errors noticeable only in the logarithmic scale. Further, our hybrid algorithm is executable on IBM quantum hardware as shown in Panel 5b. Lastly, Panel 5c shows that truncation thresholds fall within our provided upper bound in Proposition 4 in practice.

where $\Delta = \nabla^2$ is the Laplacian operator, $\Phi(x, t)$ and $f(x, t)$ are the temperature and a known heat source at the grid position of x at time t respectively. Consider an initial time constraint and a $x_R \in \mathbb{R}$ periodic spatial boundary condition,

$$\Phi(x, 0) = \phi(x); \quad \Phi(x, t) = \Phi(x + x_R, t), \quad (20)$$

where $\phi(x)$ is the initial distribution function. With the finite difference method [23], we can obtain a numerical solution to the heat transfer problem by solving the corresponding linear systems of equations in the form of $Cx = \mathbf{b}$, where x is the temperature distribution and \mathbf{b} is a known vector [34]. In this scenario, the matrix C is given by

$$C = \begin{pmatrix} -2 - \xi & 1 & 0 & \cdots & 0 & 1 \\ 1 & -2 - \xi & 1 & \ddots & \ddots & 0 \\ 0 & 1 & \ddots & \ddots & \ddots & \vdots \\ \vdots & \ddots & \ddots & \ddots & \ddots & 0 \\ 0 & \ddots & \ddots & \ddots & \ddots & 1 \\ 1 & 0 & \cdots & 0 & 1 & -2 - \xi \end{pmatrix}, \quad (21)$$

where $\xi \in \mathbb{R}$ is a grid parameter. As C is a circulant matrix, it has the form of a linear combination of cyclic permutation matrices Q and Q^{-1} , in addition to the identity matrix,

$$C = (-2 - \xi)\mathbb{I} + Q + Q^{-1}. \quad (22)$$

The condition number of the matrix in Equation 21 is shown to be $\kappa_C = \frac{\xi+4}{\xi}$ by Guseynov *et al.* [34]. Note that when $\xi \rightarrow 0$, the condition number $\kappa_C \rightarrow +\infty$.

Numerical results. To demonstrate our algorithm in practice, we perform three numerical experiments, the results of which are summarized in Figure 5.

We first examine the performance of our algorithm on simulations of solving the heat transfer problem. We set the grid parameter $\xi = 0.2$ and the system size $N = 2^5$. The input state \mathbf{b} is prepared by a single-layer QAOA circuit [35, 36] with the rotation parameters of $\{\frac{\pi}{2}, \frac{\pi}{4}, \frac{\pi}{8}, \frac{\pi}{16}, \frac{\pi}{32}\}$ as shown in Figure 4. Note that we do not tune the parameters of the circuit, but merely use its structure to prepare our quantum state. We solve the corresponding circulant linear system of equations using three methods—direct matrix multiplication, simulation of the hybrid algorithm via the `qiskit-aer` simulator with 6×10^4 shots per Hadamard test, and simulation of the quantum-inspired algorithm with 6×10^4 accesses per sampling. The results are shown in Figure 5a. We note that our algorithms can provide a close estimate to that of the true value obtained by matrix multiplication, with errors noticeable only on the logarithmic scale.

Testing the performance of the hybrid algorithm on real quantum devices, we execute our hybrid algorithm on `ibm-perth` hardware. Due to the high consumption of quantum resource of the QFT subroutine on current quantum devices, we consider a smaller size of $N = 2^3$ and set \mathbf{b} as $|0\rangle^{\otimes 3}$. We set the shot number as 10^6 . We find that on small systems, our algorithms can still produce results close to the values obtained by the matrix multiplication with the loss error not exceeding 0.05, as shown in Figure 5b.

Lastly, we compare the condition number with the truncation threshold under different input states $|b\rangle$. Setting the system size of $N = 2^{10}$, we evaluate on three different types of \mathbf{b} , the zero state $|0^{10}\rangle$, the GHZ state $|0^{10}\rangle + |1^{10}\rangle / \sqrt{2}$ and the amplitude encoded state $\sum_{k=0}^{1023} k |k\rangle / \sqrt{\sum_{k=0}^{1023} k^2}$. We tune the parameter the parameter ξ to adjust the condition number κ_C . Fixing a loss threshold $v = 10^{-2}$, we record the minimum truncation threshold T that achieves an MSE loss less than v as shown in Figure 5c. We note that from the slope of the log-log plot, we can obtain the exponent of κ_C when the truncation threshold T is modeled as a polynomial function of κ_C . We note that for the zero and GHZ state, the exponent seems to converge to a small value, suggesting the $T \in o(\kappa_C)$. Further, for the amplitude encoded state, we see that the slope is approximately $\frac{2}{3}$, indicating that $T \propto \kappa_C^{2/3}$. We note that our results all verify that the upper bound $T \in O(\kappa_C \log \kappa_C)$ provided by Proposition 4, however, we have not found a vector \mathbf{b} that saturates this upper bound, hence providing no empirical suggestions of the tightness of the proposition.

VIII. CONCLUSION

This work explores an efficient strategy to solve circulant linear systems. Two different approaches are given—a hybrid quantum-classical algorithm and a sample and query access based quantum-inspired classical algorithm. As banded circulant systems can be expanded as a matrix polynomial of the cyclic permutation matrix Q , we adapt and modify the CQS approach proposed by Huang *et al.* [7] to convert the linear systems problem into a classical convex optimization problem with lower dimensions. In replacement of iteratively growing Ansatz trees using heuristical gradient expansion strategies, we utilize the properties of circulant systems and only explore the direct sum of two Krylov subspaces $\mathcal{K}_T(Q, \mathbf{b})$ and $\mathcal{K}_T(Q^{-1}, \mathbf{b})$ to obtain our solution.

The circulant matrix provides various properties that can provide convenience for solving such systems. For the hybrid algorithm, we make use of the efficient implementation of the powers of the cyclic permutation matrix Q due to its eigendecomposition by QFT, as well as the availability of a tensor product decomposition of the diagonalized matrix Λ . For the quantum-inspired algorithm, we make use of the fact the Q evaluates to a simple shift in query indexes when applied to vector \mathbf{b} . Such properties allow our algorithm to operate under lower time complexities compared to algorithms that solve generalized linear systems of equations. Further, we show the relevancy of the hybrid algorithm by discussing the `PromiseBQP`-hardness of optimization under the hybrid setting.

To demonstrate the applicability of such algorithms in applications that require solving circulant systems, we execute our algorithm in simulations as well as quantum hardware to solve partial differential equations produced by discretizing heat transfer problems, showing that these algorithms can indeed be utilized to produce approximate solutions that are close to the optimal solution obtained by exact algorithms that require a much higher runtime. However, we note that the assumptions of preparation of vectors as a quantum state or allowing sample and query access may prevent such algorithms from universal usage and/or provide an actual advantage over current classical algorithms. Nevertheless, such algorithms provide an interesting study on circulant systems and may be used to provide potential speedups in physics-related applications.

ACKNOWLEDGMENTS

The authors would like to thank Bin Cheng for the valuable discussions and suggestions. This work is supported by the National Research Foundation, Singapore, and A*STAR under its CQT Bridging Grant and its Quantum Engineering Programme under grant NRF2021-QEP2-02-P05. XL acknowledges support from the CQT Graduate Scholarship. KK acknowledges support from Leong Chuan Kwek, under project grant R-710-000-007-135.

Appendix A: Provable performance guarantees

Proof for Proposition 4. Our proof is divided into two parts; we first discuss the case where C is Hermitian and then generalize the results to a non-Hermitian C .

C is Hermitian: Discussing the case where C is Hermitian, we first let $\hat{C} = C/\|C\|$. We find that the singular values of \hat{C} are equal to the absolute value of the eigenvalues of \hat{C} , that is, $\{\sigma_k(\hat{C})\}_{k \in [N]} = \{|\lambda_k(\hat{C})|\}_{k \in [N]}$. Further notice that $\|\hat{C}\| = 1$ and $\kappa_{\hat{C}} = \kappa_C$. Noting that the eigenvalues of \hat{C} are all real, we can see that all eigenvalues of \hat{C} fall within the domain $\mathcal{D}_{\kappa_C} = [-1, -\frac{1}{\kappa_C}] \cup [\frac{1}{\kappa_C}, 1]$, as limited by the largest and smallest singular values. Similar to the proof of proposition 4 of [7], we find that by Lemma 14 of [37], there exists a set of coefficients $j \in [0, j_0]$ such that $f(x) = \sum_{j=0}^{j_0} p_j x^j$ where $j_0 = \sqrt{\beta \log \frac{4\beta}{\nu}}$ and $\beta = \kappa_C^2 \log \frac{\kappa_C}{\nu}$, such that $f(x)$ is 2ν -close to x^{-1} on domain \mathcal{D}_{κ_C} . We can obtain by diagonalization of powers of \hat{C} that

$$\|f(\hat{C}) - \hat{C}^{-1}\| = \max_{i \in [N]} \sigma_i(f(\hat{C}) - \hat{C}^{-1}) = \max_{i \in [N]} |\lambda_i(f(\hat{C}) - \hat{C}^{-1})| = \max_{i \in [N]} |f(\lambda_i(\hat{C})) - \lambda_i(\hat{C})^{-1}| \leq 2\nu. \quad (\text{A1})$$

Let $g(x) = \sum_{j=0}^{j_0} \frac{p_j}{\|C\|^{j+1}} x^j$. Note that

$$\|g(C) - C^{-1}\| = \left\| \sum_{j=0}^{j_0} \frac{p_j}{\|C\|^{j+1}} C^j - C^{-1} \right\| = \left\| \sum_{j=0}^{j_0} \frac{p_j}{\|C\|} \hat{C}^j - \frac{1}{\|C\|} \hat{C}^{-1} \right\| = \frac{1}{\|C\|} \|f(\hat{C}) - \hat{C}^{-1}\| \leq \frac{2\nu}{\|C\|} \quad (\text{A2})$$

Recall that $C = \sum_{\ell=-K}^K c_\ell Q^\ell$. Let $T = j_0 K \in O(K \cdot \kappa_C \log \frac{\kappa_C}{\nu})$. We can find that there exists a set of parameters $\{\hat{\alpha}_i : i \in [-T..T], \hat{\alpha}_i \in \mathbb{C}\}$ such that $g(C) = \sum_{j=0}^{j_0} \frac{p_j}{\|C\|^{j+1}} C^j = \sum_{m=-T}^T \hat{\alpha}_m Q^m$. We then find that

$$\min_{\{\alpha_m\}_{m \in [-T..T]}} \left\| C \left(\sum_{m=-T}^T \alpha_m Q^m \right) \mathbf{b} - \mathbf{b} \right\|^2 \leq \left\| C \left(\sum_{m=-T}^T \hat{\alpha}_m Q^m \right) \mathbf{b} - \mathbf{b} \right\|^2 = \|Cg(C)\mathbf{b} - \mathbf{b}\|^2 \quad (\text{A3})$$

We now observe the following:

$$\|Cg(C)\mathbf{b} - \mathbf{b}\|^2 = \|(C(g(C) - C^{-1})\mathbf{b}) + (CC^{-1}\mathbf{b} - \mathbf{b})\|^2 \quad (\text{A4})$$

$$= \|C(g(C) - C^{-1})\mathbf{b}\|^2 + \|CC^{-1}\mathbf{b} - \mathbf{b}\|^2 + 2 \operatorname{Re} \langle C(g(C) - C^{-1})\mathbf{b}, CC^{-1}\mathbf{b} - \mathbf{b} \rangle \quad (\text{A5})$$

Given that $\langle C(g(C) - C^{-1})\mathbf{b}, CC^{-1}\mathbf{b} - \mathbf{b} \rangle = \langle (g(C) - C^{-1})\mathbf{b}, C^\dagger CC^{-1}\mathbf{b} - C^\dagger \mathbf{b} \rangle = \langle (g(C) - C^{-1})\mathbf{b}, C^\dagger \mathbf{b} - C^\dagger \mathbf{b} \rangle = 0$, we have

$$\|Cg(C)\mathbf{b} - \mathbf{b}\|^2 = \|CC^{-1}\mathbf{b} - \mathbf{b}\|^2 + \|C(g(C) - C^{-1})\mathbf{b}\|^2. \quad (\text{A6})$$

Observe that the first term is the MSE loss of the least-squares solution of $x = C^{-1}\mathbf{b}$ and can hence be rewritten as $\min_{x \in \mathbb{C}^N} \|Cx - \mathbf{b}\|^2$.

The spectral norm of matrix A can be defined by vector 2-norms such that

$$\|A\| = \sup_{x \neq 0} \frac{\|Ax\|}{\|x\|}, \quad (\text{A7})$$

Hence one can obtain inequality

$$\|Ax\| \leq \|A\| \|x\|. \quad (\text{A8})$$

We then see that the second term $\|C(g(C) - C^{-1})\mathbf{b}\|^2$ can be upper bounded as follows:

$$\|C(g(C) - C^{-1})\mathbf{b}\|^2 \leq \|C\|^2 \|(g(C) - C^{-1})\mathbf{b}\|^2 \leq \|C\|^2 \|g(C) - C^{-1}\|^2 \|\mathbf{b}\|^2 = \|C\|^2 \frac{4\nu^2}{\|C\|^2} \leq 4\nu^2 \leq 4\nu, \quad (\text{A9})$$

with the last inequality using the fact that $0 < \nu \leq 1$. Hence we note that the solution obtained by our truncation threshold $T \in O(K \cdot \kappa_C \log \frac{\kappa_C}{\nu})$ has

$$\min_{\{\alpha_m\}_{m \in [-T..T]}} \left\| C \left(\sum_{m=-T}^T \alpha_m Q^m \right) \mathbf{b} - \mathbf{b} \right\|^2 \leq \min_{x \in \mathbb{C}^N} \|Cx - \mathbf{b}\|^2 + 4\nu \quad (\text{A10})$$

C is non-Hermitian: Consider the following transformation and embedding matrices:

$$C' = \begin{pmatrix} O & C \\ C^\dagger & O \end{pmatrix} \quad \mathbf{b}' = \begin{pmatrix} \mathbf{b} \\ 0 \end{pmatrix} \quad x' = \begin{pmatrix} 0 \\ x \end{pmatrix}. \quad (\text{A11})$$

Through the embedding, we can transform our linear system into solving $C'x' = \mathbf{b}'$ where C' is now Hermitian. We know that the eigenvalues of C' correspond to the set $\{\pm\sigma_k(C)\}_{\forall k \in [N]}$ [1]. Hence the singular values of C' are equal to the set of singular values of C . Thus we have $\kappa_{C'} = \kappa_C$ and $\|C'\| = \|C\|$. Constructing $\hat{C}' = \frac{C'}{\|C\|}$, we see all eigenvalues of \hat{C}' fall within the domain $\mathcal{D}_{\kappa_C} = [-1, -\frac{1}{\kappa_C}] \cup [\frac{1}{\kappa_C}, 1]$.

By Lemma 14 of [37] and Equation A2, we see that exists $g(x) = \sum_{j=0}^{j_0} \frac{p_j}{\|C\|^{j+1}} x^j$ such that

$$\|g(C') - C'^{-1}\| \leq \frac{2\nu}{\|C'\|}, \quad (\text{A12})$$

To find a decomposition of C' , we first find the decomposition of C^\dagger . Using the fact that Q is unitary, thus the adjoint/transpose of Q^m is Q^{-m} :

$$C^\dagger = \left(\sum_{\ell=-K}^K c_\ell Q^\ell \right)^\dagger = \sum_{\ell=-K}^K \bar{c}_\ell Q^{-\ell} = \sum_{\ell=-K}^K \bar{c}_{-\ell} Q^\ell, \quad (\text{A13})$$

where \bar{c}_ℓ is the conjugate of c_ℓ . We can then express C' as follows

$$C' = \begin{pmatrix} O & C \\ C^\dagger & O \end{pmatrix} = \begin{pmatrix} O & \sum_{\ell=-K}^K c_\ell Q^\ell \\ \sum_{\ell=-K}^K \bar{c}_{-\ell} Q^\ell & O \end{pmatrix} = \sum_{\ell=-K}^K \begin{pmatrix} 0 & c_\ell \\ \bar{c}_{-\ell} & 0 \end{pmatrix} \otimes Q^\ell \quad (\text{A14})$$

One can find that for $T \in O(K \cdot \kappa \log \frac{\kappa}{\nu})$, there exists a set of parameters such that $\{\hat{\alpha}_m, \hat{\beta}_m, \hat{\gamma}_m, \hat{\delta}_m : m \in [-T..T], \hat{\alpha}_i, \hat{\beta}_m, \hat{\gamma}_m, \hat{\delta}_m \in \mathbb{C}\}$ such that we can write $g(C')$ in the following form:

$$g(C') = \sum_{j=0}^{j_0} \frac{p_j}{\|C\|^{j+1}} C'^j = \sum_{j=0}^{j_0} \frac{p_j}{\|C\|^{j+1}} \left(\sum_{\ell=-K}^K \begin{pmatrix} 0 & c_\ell \\ \bar{c}_{-\ell} & 0 \end{pmatrix} \otimes Q^\ell \right)^j \quad (\text{A15})$$

$$= \sum_{m=-T}^T \begin{pmatrix} \hat{\beta}_i & \hat{\delta}_m \\ \hat{\alpha}_m & \hat{\gamma}_m \end{pmatrix} \otimes Q^m = \begin{pmatrix} \sum_{m=-T}^T \hat{\beta}_m Q^m & \sum_{m=-T}^T \hat{\delta}_m Q^m \\ \sum_{m=-T}^T \hat{\alpha}_m Q^m & \sum_{m=-T}^T \hat{\gamma}_m Q^m \end{pmatrix} \quad (\text{A16})$$

Furthermore, observe that the following equality is true:

$$C'g(C')\mathbf{b}' = \begin{pmatrix} O & C \\ C^\dagger & O \end{pmatrix} \begin{pmatrix} \sum_{m=-T}^T \hat{\beta}_m Q^m & \sum_{m=-T}^T \hat{\delta}_m Q^m \\ \sum_{m=-T}^T \hat{\alpha}_m Q^m & \sum_{m=-T}^T \hat{\gamma}_m Q^m \end{pmatrix} \begin{pmatrix} \mathbf{b} \\ 0 \end{pmatrix} \quad (\text{A17})$$

$$= \begin{pmatrix} C \sum_{m=-T}^T \hat{\alpha}_m Q^m & C \sum_{m=-T}^T \hat{\gamma}_m Q^m \\ C^\dagger \sum_{m=-T}^T \hat{\beta}_m Q^m & C^\dagger \sum_{m=-T}^T \hat{\delta}_m Q^m \end{pmatrix} \begin{pmatrix} \mathbf{b} \\ 0 \end{pmatrix} = \begin{pmatrix} C \left(\sum_{m=-T}^T \hat{\alpha}_m Q^m \right) \mathbf{b} \\ C^\dagger \left(\sum_{m=-T}^T \hat{\beta}_m Q^m \right) \mathbf{b} \end{pmatrix} \quad (\text{A18})$$

We now attempt to upper bound the MSE loss obtained from our estimator $\tilde{x} = \sum_{m=-T}^T \alpha_m Q^m$:

$$\min_{\{\alpha_m\}_{m \in [-T..T]}} \left\| C \left(\sum_{m=-T}^T \alpha_m Q^m \right) \mathbf{b} - \mathbf{b} \right\|^2 \leq \left\| C \left(\sum_{m=-T}^T \hat{\alpha}_m Q^m \right) \mathbf{b} - \mathbf{b} \right\|^2 = \left\| \begin{pmatrix} C \left(\sum_{m=-T}^T \hat{\alpha}_m Q^m \right) \mathbf{b} \\ 0 \end{pmatrix} - \begin{pmatrix} \mathbf{b} \\ 0 \end{pmatrix} \right\|^2 \quad (\text{A19})$$

$$\leq \left\| \begin{pmatrix} C \left(\sum_{m=-T}^T \hat{\alpha}_m Q^m \right) \mathbf{b} \\ C^\dagger \left(\sum_{m=-T}^T \hat{\beta}_m Q^m \right) \mathbf{b} \end{pmatrix} - \begin{pmatrix} \mathbf{b} \\ 0 \end{pmatrix} \right\|^2 \leq \|C' g(C') \mathbf{b}' - \mathbf{b}'\|^2, \quad (\text{A20})$$

where the second-to-last inequality can be obtained by simply observing the fact that replacing zero terms in a vector with non-zero terms increases the value of the ℓ_2 norm, and the last equality is obtained by replacing the term $\begin{pmatrix} C \left(\sum_{m=-T}^T \hat{\alpha}_m Q^m \right) \mathbf{b} & C^\dagger \left(\sum_{m=-T}^T \hat{\beta}_m Q^m \right) \mathbf{b} \end{pmatrix}^\top$ with $C' g(C') \mathbf{b}'$.

Similar to the Hermitian case, we obtain the following:

$$\|C' g(C') \mathbf{b}' - \mathbf{b}'\|^2 = \|C' C'^{-1} \mathbf{b}' - \mathbf{b}'\|^2 + \|C' (g(C') - C'^{-1}) \mathbf{b}'\|^2. \quad (\text{A21})$$

Noting that $C'^{-1} = \begin{pmatrix} O & C^{\dagger-1} \\ C^{-1} & O \end{pmatrix}$, we can recast the first term as follows:

$$\|C' C'^{-1} \mathbf{b}' - \mathbf{b}'\|^2 = \left\| \begin{pmatrix} O & C \\ C^\dagger & O \end{pmatrix} \begin{pmatrix} O & C^{\dagger-1} \\ C^{-1} & O \end{pmatrix} \mathbf{b}' - \mathbf{b}' \right\|^2 = \left\| \begin{pmatrix} C C^{-1} & O \\ O & C^\dagger C^{\dagger-1} \end{pmatrix} \begin{pmatrix} \mathbf{b} \\ 0 \end{pmatrix} - \begin{pmatrix} \mathbf{b} \\ 0 \end{pmatrix} \right\|^2 \quad (\text{A22})$$

$$= \left\| \begin{pmatrix} C C^{-1} \mathbf{b} \\ 0 \end{pmatrix} - \begin{pmatrix} \mathbf{b} \\ 0 \end{pmatrix} \right\|^2 = \|C C^{-1} \mathbf{b} - \mathbf{b}\|^2 = \min_{x \in \mathbb{C}^N} \|C x - \mathbf{b}\|^2 \quad (\text{A23})$$

As $\|\mathbf{b}'\| = 1$, the second term is upper bounded as follows:

$$\|C' (g(C') - C'^{-1}) \mathbf{b}'\|^2 \leq \|C'\|^2 \|g(C') - C'^{-1}\|^2 \|\mathbf{b}'\|^2 = \|C'\|^2 \frac{4\nu^2}{\|C\|^2} \leq 4\nu^2 \leq 4\nu \quad (\text{A24})$$

Hence we see that for the non-Hermitian case, the solution obtained by our truncation threshold $T \in \mathcal{O}(K \cdot \kappa_C \log \frac{\kappa_C}{\nu})$ is still ν -close in terms of the MSE loss. \square

Appendix B: Quantum subroutines

In the following section, we provide brief reviews of quantum subroutines used in our paper.

Hadamard test. Hadamard tests [22] are used as a method to obtain a random variable whose expectation value is the real (or imaginary) part of $\langle \psi | U | \psi \rangle$, where $|\psi\rangle$ is a quantum state and U is unitary. Given an additional ancilla qubit, one can prepare the controlled version of U and run the quantum circuit given by Figure 6a for finding the real part and Figure 6b for finding the imaginary part. To compute the expectation value, obtain the probability of measuring 1 minus the probability of measuring 0. Invert the sign when obtaining the imaginary part. Note that the expected values produced by Hadamard test have additive accuracy ε with failure probability at most δ using $\mathcal{O}\left(\frac{1}{\varepsilon^2} \log\left(\frac{1}{\delta}\right)\right)$ measurements, which can be shown using Hoeffding's inequality.

Quantum Fourier transform. Given $N = 2^n$, the quantum Fourier transform [17] performs the following transformation on a quantum state:

$$|b\rangle = \sum_{x=0}^{N-1} b_x |x\rangle \longrightarrow \frac{1}{\sqrt{N}} \underbrace{\sum_{x=0}^{N-1} b_x \omega_N^{xy} |y\rangle}_{F_N |b\rangle}. \quad (\text{B1})$$

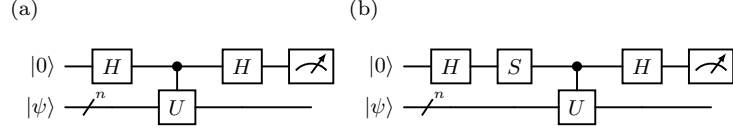


FIG. 6. Circuit implementation of the Hadamard test. Panel 6a is the circuit for retrieving $\text{Re} \langle \psi | U | \psi \rangle$, while Panel 6b is the circuit for retrieving $\text{Im} \langle \psi | U | \psi \rangle$.

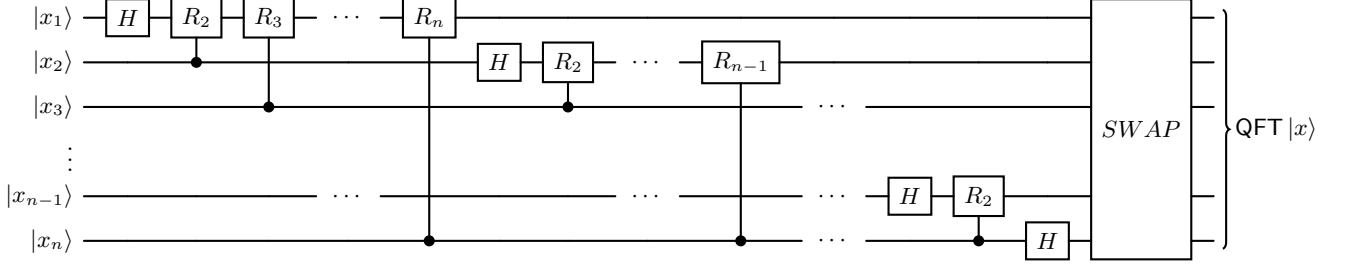


FIG. 7. Implementation of the quantum Fourier transform, where the final SWAP gate reverses the order of qubits.

Given the following gate:

$$R_k = \begin{pmatrix} 1 & 0 \\ 0 & \omega_N^k \end{pmatrix}, \quad (\text{B2})$$

QFT can be implemented as Figure 7.

Arbitrary sized quantum Fourier transform. The quantum Fourier transform as proposed by Coppersmith [17] is implemented as a unitary acting on n qubits, which makes it an operator of size $2^n \times 2^n$. Here, we consider the case where we are interested in discrete Fourier transforming a vector of N -amplitudes, where $2^{n-1} < N < 2^n$ for some n . This generalized QFT, first conceived of as an approximation by Kitaev [32] and made exact by Mosca and Zalka [38], makes use of quantum phase estimation (QPE) proposed in the former paper, which itself incorporates the ‘standard’ QFT by Coppersmith [17]

First, an amplitude- N vector can be stored using n -qubits if $N < 2^n$ by preparing the quantum state as a superposition of $|0\rangle$ to $|N-1\rangle$. Denote the size- N discrete Fourier transform by F_N , and the quantum circuit implementing it by QFT_N . By definition,

$$F_N |x\rangle = \frac{1}{\sqrt{N}} \sum_{y=0}^{N-1} \omega_N^{xy} |y\rangle \quad (\text{B3})$$

over the basis states $|x\rangle$ and extending by linearity.

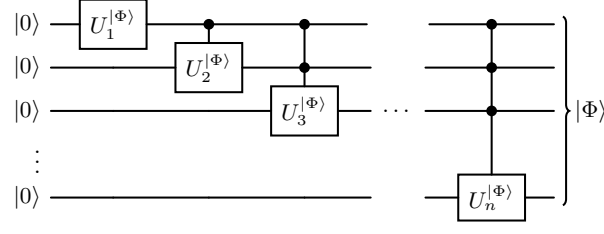
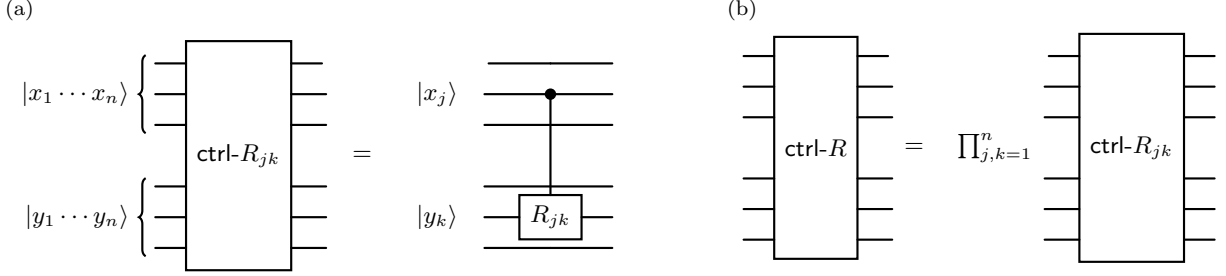
Let $|b\rangle = \sum_{x=0}^{N-1} b_x |x\rangle$, and let $|0\rangle$ denote the ancilla qubits. Kitaev’s method proceeds along the following sequence of transformations: for general $|b\rangle$,

$$|b\rangle \otimes |0\rangle \xrightarrow{\text{condRot}} \sum_x b_x |x\rangle \otimes \underbrace{\frac{1}{\sqrt{N}} \sum_{y=0}^{N-1} |y\rangle}_{=F_N|0\rangle} \xrightarrow{\text{ctrl-R}} \sum_x b_x |x\rangle \otimes \underbrace{\frac{1}{\sqrt{N}} \sum_{y=0}^{N-1} \omega_N^{xy} |y\rangle}_{=F_N|x\rangle} \xrightarrow{\text{QPE}^{-1}} |0\rangle \otimes \underbrace{\sum_x b_x |\Phi_x\rangle}_{=F_N|b\rangle}. \quad (\text{B4})$$

Note how the last transformation is necessary to isolate the Fourier transform of $|b\rangle$. Let us now see how to implement the transformations condRot , ctrl-R , and QPE^{-1} .

To implement condRot , let us consider the construction of the more general state taking the form

$$|\Phi\rangle = \sum_{x=0}^{N-1} a_x |x\rangle = \sum_{x_1, \dots, x_n \in \{0,1\}} a_{x_1 \dots x_n} |x_1 \dots x_n\rangle \quad (\text{B5})$$

FIG. 8. Implementation of condRot in Equation B4.FIG. 9. Implementation of transformation ctrl-R in Equation B4. Panel 9a shows the actual gate of ctrl-R_{jk} , while Panel 9b shows the implementation of ctrl-R as a product of the all possible ctrl-R_{jk} operations. Note that the order of implementation does not matter as these operations commute with each other.

where $0 \leq a_{x_1 \dots x_n} \in \mathbb{R}$. $F_N |0\rangle$ is the special case when $a_x = \frac{1}{\sqrt{N}}$ for $0 \leq x \leq N-1$, $a_x = 0$ for $x \geq N$. The probability of a sequence of events occurring can be factored into a product of conditional probabilities of the subevents occurring. Since the probability amplitudes in this state are all nonnegative real numbers, the *probability amplitudes* themselves can be factored—this corresponds to taking the square root of the equation above, i.e. $a_{x_1 x_2 \dots x_n} = a_{x_1} a_{x_2 | x_1} a_{x_3 | x_2 x_1} \dots$. We distribute the factor $a_{x_k | x_{k-1} \dots x_1}$ to the corresponding k -th qubit.

We begin by initializing the n -qubit state to $|0^n\rangle$. If we measure $|\Phi\rangle$ in the computational basis, the probability of getting $x_1 = 0$ for the first qubit is $\sum_{x_2, \dots, x_n \in \{0,1\}} a_{0, x_2, \dots, x_n}^2$. Denote this by a_0^2 and similarly define a_1^2 . The first operation to perform is on the first qubit, where

$$|0\rangle \rightarrow a_0 |0\rangle + a_1 |1\rangle. \quad (\text{B6})$$

The map here is so far only defined for $|0\rangle$, but we can choose its action arbitrarily on $|1\rangle$ as long as the unitary constraint is respected. In what follows we shall apply this fact repeatedly, and omit any further mention of the maps' action on $|1\rangle$ states. Next, the probability of getting $x_2 = 0$ is $\sum_{x_3, \dots, x_n \in \{0,1\}} a_{0,0, x_3, \dots, x_n}^2$ —denote this by $a_{0|0}^2$ and similarly for $a_{1|0}^2$. Thus the next operation to apply is the conditional rotation on the second qubit:

$$|x_1, 0\rangle \rightarrow a_{0|x_1} |0\rangle + a_{1|x_1} |1\rangle. \quad (\text{B7})$$

Carrying on in this manner, we see that the k -th operation on the k -th qubit is controlled by the previous $k-1$ qubits:

$$|x_1, \dots, x_{k-1}, 0\rangle \rightarrow |x_1, \dots, x_{k-1}\rangle \otimes (a_{0|x_1 \dots x_{k-1}} |0\rangle + a_{1|x_1 \dots x_{k-1}} |1\rangle). \quad (\text{B8})$$

It is observed that the probability amplitude of the final (highly superposed) state to be in state $|x_1 x_2 \dots x_n\rangle$ is $a_{x_1} a_{x_2 | x_1} \dots a_{x_n | x_{n-1} \dots x_1} = a_{x_1 \dots x_n}$, as expected.

ctrl-R can be implemented with a series of controlled phase shifts, which is very similar to the subroutine used in the usual QFT. We only need to demonstrate how to implement $|x\rangle |y\rangle \rightarrow \omega_N^{xy} |x\rangle |y\rangle$; linearity will complete the argument. Recall that a positive integer $x = \sum_{k=1}^n x_k 2^{n-k}$ is represented in binary as $x = x_1 x_2 \dots x_n$. Given $x = \sum_{k=1}^n x_k 2^{n-k}$, $y = \sum_{k=1}^n y_k 2^{n-k}$, we have $xy = \sum_{j,k=1}^n x_j y_k \cdot 2^{2n-(j+k)}$.

Thus define the phase gate

$$R_{jk} = \begin{bmatrix} 1 & 0 \\ 0 & \omega_N^{2^{2n-(j+k)}} \end{bmatrix}. \quad (\text{B9})$$

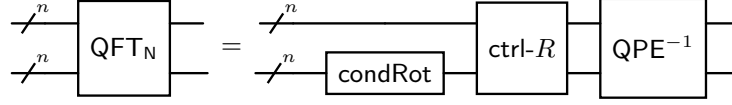


FIG. 10. Full implementation of arbitrary sized discrete Fourier transform F_N . $\text{QFT}_N |b\rangle \otimes |0^n\rangle = |0^n\rangle \otimes F_N |b\rangle$.

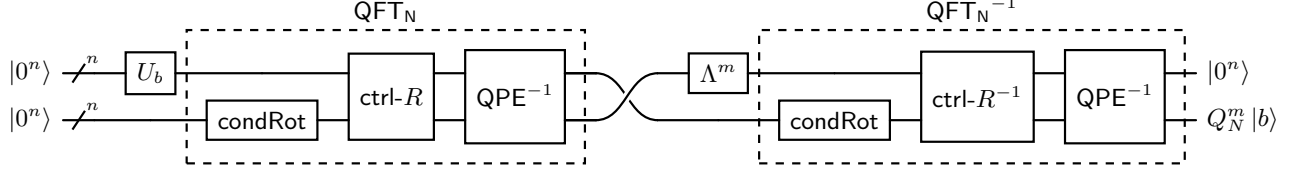


FIG. 11. Quantum circuit constructing $Q_N^m |b\rangle$ as discussed in the main text.

If we control this phase gate by $|x_j\rangle$ and let it act on $|y_k\rangle$, the resulting gate is

$$\text{ctrl-}R_{jk} = |0\rangle\langle 0|_j \otimes I_k + |1\rangle\langle 1|_j \otimes \left(|0\rangle\langle 0|_k + \omega_N^{2^{2n-(j+k)}} |1\rangle\langle 1|_k \right). \quad (\text{B10})$$

Here for notational simplicity, we have omitted the identities acting on all the other qubits $|x_{j'}\rangle, j' \neq j$ and $|y_{k'}\rangle, k' \neq k$. The action of this operator on $|x\rangle |y\rangle = |x_1 \dots x_n\rangle |y_1 \dots y_n\rangle$ is

$$\begin{aligned} \text{ctrl-}R_{jk} |x_1 \dots x_n\rangle |y_1 \dots y_n\rangle &= \delta_{x_j,0} |x_1 \dots 0_j \dots x_n\rangle |y_1 \dots y_n\rangle + \\ &\quad \delta_{x_j,1} |x_1 \dots 1_j \dots x_n\rangle \otimes \left(\delta_{y_k,0} |y_1 \dots 0_k \dots y_n\rangle + \omega_N^{2^{2n-(j+k)}} \delta_{y_k,1} |y_1 \dots 1_k \dots y_n\rangle \right) \end{aligned} \quad (\text{B11})$$

$$= \delta_{x_j,0} |x_1 \dots 0_j \dots x_n\rangle |y_1 \dots y_n\rangle + \delta_{x_j,1} |x_1 \dots 1_j \dots x_n\rangle \otimes \omega_N^{y_k \cdot 2^{2n-(j+k)}} |y_1 \dots y_n\rangle \quad (\text{B12})$$

$$= \omega_N^{x_j y_k \cdot 2^{2n-(j+k)}} |x_1 \dots x_n\rangle |y_1 \dots y_n\rangle. \quad (\text{B13})$$

By applying $\text{ctrl-}R_{jk}$, we create a phase factor of $\omega_N^{x_j y_k \cdot 2^{2n-(j+k)}}$, which is a summand in the binary expansion of xy . Applying $\text{ctrl-}R := \prod_{j,k=1}^n \text{ctrl-}R_{jk}$ therefore gives us the desired phase factor ω_N^{xy} .

QPE^{-1} is a straightforward application: since $|0\rangle \otimes F_N |x\rangle \rightarrow |x\rangle \otimes F_N |x\rangle$ via quantum phase estimation (here, the $F_N |x\rangle$ s are eigenvectors of the unitary defined by $U |x\rangle = |x-1 \pmod N\rangle$), the map implementing $T3$ is simply the inverse of QPE , which we denote by QPE^{-1} .

Lastly, we discuss the steps to prepare $Q_N^m |b\rangle = \text{QFT}_N^{-1} \Lambda^m \text{QFT}_N^{-1}$. Λ^m can be implemented by retaining the phase gate structure and setting ω_N to correspond to N instead of the quantum system size. Note that because the Fourier transform and its inverse differ only in the -1 phase in the coefficient exponents, the procedure for implementing the inverse Fourier transform is essentially the same as that for the original transform, the only difference coming from the controlled phase gates. For QFT_N^{-1} , the phase gates used are

$$R_{kl}^{-1} = \begin{bmatrix} 1 & 0 \\ 0 & \omega_N^{-2^{2n-(k+l)}} \end{bmatrix}. \quad (\text{B14})$$

We denote their product by $\text{ctrl-}R^{-1} = \prod_{k,l=1}^n \text{ctrl-}R_{kl}^{-1}$.

The circuit for constructing the Ansatz states $Q_N^m |b\rangle$ is shown in Figure 11. Note that only one set of n ancillary qubits is required.

Appendix C: Complexity of optimization problem

To show the hardness of our `QUANTUMCIRCULANTOPTIM` problem, we first discuss a problem introduced by Aaronson [39] known as `FORRELATION` [40] or `FOURIER-CHECKING`. In particular, it has been shown that a variant of `FORRELATION` known as k -fold `FORRELATION` is `PromiseBQP`-complete.

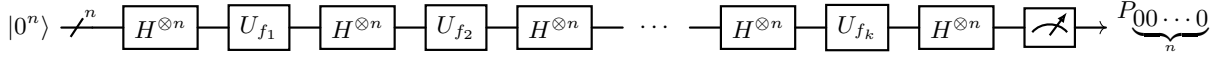


FIG. 12. Quantum algorithm given by Aaronson and Ambainis [40] to solve the k -fold FORRELATION problem. The first WHT is used to create a superposition state over all states in the computational basis, the WHTs in between are used to create a Fourier transform, while the last WHT transforms measurement over the Pauli-X basis to measurement over the Pauli-Z basis. Oracles $U_{f_1}, U_{f_2}, \dots, U_{f_k}$ are used to implement the functions $f_1(\cdot), f_2(\cdot), \dots, f_k(\cdot)$.

In FORRELATION, two functions $f, g \in \{0, 1\}^n \rightarrow \{-1, 1\}$ are given. The correlation between the Fourier transform of f and g , or forrelation, is computed as follows:

$$\Phi_{f,g} := \frac{1}{2^{3n/2}} \sum_{x,y \in \{0,1\}^n} f(x)(-1)^{x \cdot y} g(y) \quad (\text{C1})$$

Note that the Fourier transform here refers to the Walsh-Hadamard transform (WHT) implemented by the tensor product of n Hadamard gates instead of DFT implemented by the QFT circuit due to the consideration of the n -qubit system as the boolean group $(\mathbb{Z}/2\mathbb{Z})^n$ instead of the cyclic group $\mathbb{Z}/2^n\mathbb{Z}$. Given the promise that $|\Phi_{f,g}|$ is either less than $\frac{1}{100}$ or greater than $\frac{3}{5}$, FORRELATION is a decision problem that differentiates between the two cases.

In the k -fold FORRELATION variant introduced by Aaronson and Ambainis [40], k functions $f_1, f_2, \dots, f_k \in \{0, 1\}^n \rightarrow \{-1, 1\}$ are given. The forrelation is calculated as follows:

$$\Phi_{f_1, f_2, \dots, f_k} := \frac{1}{2^{(k+1)n/2}} \sum_{x_1, x_2, \dots, x_k \in \{0,1\}^n} f_1(x_1)(-1)^{x_1 \cdot x_2} f_2(x_2)(-1)^{x_2 \cdot x_3} \dots (-1)^{x_{k-1} \cdot x_k} f_k(x_k) \quad (\text{C2})$$

Given the promise that $|\Phi_{f_1, f_2, \dots, f_k}|$ is either less than $\frac{1}{100}$ or greater than $\frac{3}{5}$, the k -fold FORRELATION is a decision problem that differentiates between the two cases.

Suppose that we are given oracles $U_{f_1}, U_{f_2}, \dots, U_{f_k}$ such that for any input computational basis state $|x\rangle$ where $x \in \{0, 1\}^n$, $U_{f_j}|x\rangle = f_j(x)|x\rangle$. Using these oracles, a quantum algorithm can be given such that FORRELATION can be solved with a bounded probability of error using only k quantum queries to f_1, f_2, \dots, f_k , as illustrated in Figure 12. First, prepare a uniform superposition state over all $x \in \{0, 1\}^n$. Then alternate between querying U_{f_j} in order of U_{f_1} to U_{f_k} and applying WHT until U_{f_k} is queried. Lastly, measure the probability of recovering the uniform superposition state, i.e. measuring on the Pauli-X basis for all qubits, or measuring on the Pauli-Z basis after applying the Hadamard transform on all qubits. We note that the probability of obtaining the measurement result $00 \dots 0$ is $|\Phi_{f_1, f_2, \dots, f_k}|$.

Aaronson and Ambainis [40] also proposed an alternate algorithm that replaces the direct measurement on the Pauli-Z basis with the modified Hadamard test. We omit this algorithm as we do not utilize the algorithm in the later proof. However, it is easy to see in the Hadamard test setup that k -fold FORRELATION is in **PromiseBQP** due to its single qubit measurement. Further, it has been proved that when $k = \text{poly } n$, k -fold FORRELATION is **PromiseBQP**-complete. We now show in the following that k -fold FORRELATION can be reduced to **QUANTUMCIRCULANTOPTIM**, hence showing that **QUANTUMCIRCULANTOPTIM** is **PromiseBQP**-hard.

Proof of Proposition 11. Given a k -fold FORRELATION problem acting on n qubits, we assume we have access to oracles $U_{f_1}, U_{f_2}, \dots, U_{f_k}$. We construct a banded circulant linear system of dimension 2^{n+1} , with the qubit representing the least significant bit in the computational basis being the extra qubit. Let the matrix C be the cyclic permutation matrix Q over dimension 2^{n+1} . We also give the following three quantum states:

$$|b\rangle = H^{\otimes n} U_{f_k} H^{\otimes n} U_{f_{k-1}} H^{\otimes n} \dots H^{\otimes n} U_{f_1} H^{\otimes n} |0^n\rangle \otimes |1\rangle, \quad |u_1\rangle = |0^{n+1}\rangle, \quad |u_2\rangle = |1^{n+1}\rangle \quad (\text{C3})$$

We see that when applying matrix C to the Ansatz set, we obtain the following:

$$C|u_1\rangle = |0^n\rangle \otimes |1\rangle, \quad C|u_2\rangle = |0^n\rangle \otimes |0\rangle \quad (\text{C4})$$

We can see that $\langle b|C|u_1\rangle$ evaluates to $\Phi_{f_1, f_2, \dots, f_k} \cdot 1 = \Phi_{f_1, f_2, \dots, f_k}$ while $\langle b|C|u_2\rangle$ evaluates to $\Phi_{f_1, f_2, \dots, f_k} \cdot 0 = 0$. Further note that $\langle u_1|C^\dagger C|u_2\rangle = \langle u_1|u_2\rangle = 0$.

Suppose there exists an algorithm \mathcal{A} that solves the **QUANTUMCIRCULANTOPTIM** problem with error rate $\zeta \leq \frac{1}{16}$. We now show that $\hat{\alpha}_1$ can be used to infer $\psi_{f,g}$. By expansion, we have

$$\|C(\alpha_1 |u_1\rangle + \alpha_2 |u_2\rangle) - |b\rangle\|^2 = |\alpha_1|^2 + |\alpha_2|^2 - 2 \text{Re}\{\alpha_1 \langle b|C|u_1\rangle + \alpha_2 \langle b|C|u_2\rangle\} + 1 \quad (\text{C5})$$

$$= |\alpha_1 - \Phi_{f_1, f_2, \dots, f_k}|^2 + |\alpha_2 - 0|^2 + (1 - |\Phi_{f_1, f_2, \dots, f_k}|^2) \quad (\text{C6})$$

We plug in the solution $\hat{\alpha}_1$ and $\hat{\alpha}_2$ obtained by algorithm \mathcal{A} , and find that

$$|\hat{\alpha}_1 - \Phi_{f_1, f_2, \dots, f_k}|^2 + |\hat{\alpha}_2 - 0|^2 + (1 - |\Phi_{f_1, f_2, \dots, f_k}|^2) \leq 1 - |\psi_{f, g}|^2 + \zeta \Rightarrow |\hat{\alpha}_1 - \Phi_{f_1, f_2, \dots, f_k}|^2 + |\hat{\alpha}_2 - 0|^2 \leq \zeta \quad (\text{C7})$$

Note that this gives us $|\hat{\alpha}_1 - \Phi_{f_1, f_2, \dots, f_k}|^2 \leq \zeta$. By reverse triangular inequality, we can further obtain

$$||\hat{\alpha}_1| - |\Phi_{f_1, f_2, \dots, f_k}||^2 \leq |\hat{\alpha}_1 - \Phi_{f_1, f_2, \dots, f_k}|^2 \leq \zeta \leq \frac{1}{16} \Rightarrow ||\hat{\alpha}_1| - |\Phi_{f_1, f_2, \dots, f_k}|| \leq \sqrt{\zeta} \leq \frac{1}{4}. \quad (\text{C8})$$

Hence, we see that the value of $|\hat{\alpha}_1|$ is $1/4$ -close to $|\Phi_{f_1, f_2, \dots, f_k}|$. Given the promise that $|\Phi_{f_1, f_2, \dots, f_k}|$ is either $\geq \frac{3}{5}$ or $\leq \frac{1}{100}$, if $|\hat{\alpha}| \geq \frac{7}{20}$, then $|\Phi_{f_1, f_2, \dots, f_k}| \geq \frac{3}{5}$; If $|\hat{\alpha}| \leq \frac{13}{50}$, then $|\Phi_{f_1, f_2, \dots, f_k}| \leq \frac{1}{100}$. We see that k -fold FORRELATION can be reduced to QUANTUMCIRCULANTOPTIM.

If there exists a relativizing classical algorithm that can solve QUANTUMCIRCULANTOPTIM in $\text{poly}(\kappa_C, n)$ time, the same algorithm can solve k -fold FORRELATION equally efficiently, implying that $\text{PromiseBQP} = \text{PromiseBPP}$. \square

Lastly, we note that the above proof works under the assumption that oracles and poly n depth circuits are allowed in the preparation of U_b in QUANTUMCIRCULANTOPTIM. If only poly $\log n$ depth is allowed for the preparation for U_b , only under the case where $k \in \text{poly} \log n$ is k -fold FORRELATION reducible to QUANTUMCIRCULANTOPTIM. In this case, and disregarding the implementation depth of oracles, k -fold FORRELATION is QNC-complete, and we obtain the result that QUANTUMCIRCULANTOPTIM is PromiseQNC-hard. Similarly, if there exists a classical algorithm that can solve QUANTUMCIRCULANTOPTIM efficiently, the same algorithm can solve FORRELATION equally efficiently, which implies that $\text{PromiseQNC} \subseteq \text{PromiseBPP}$.

-
- [1] A. W. Harrow, A. Hassidim, and S. Lloyd, Quantum algorithm for linear systems of equations, *Phys. Rev. Lett.* **103**, 150502 (2009).
 - [2] M. Cerezo, A. Arrasmith, R. Babbush, S. C. Benjamin, S. Endo, K. Fujii, J. R. McClean, K. Mitarai, X. Yuan, L. Cincio, and P. J. Coles, Variational quantum algorithms, *Nature Reviews Physics* **3**, 625 (2021).
 - [3] X. Xu, J. Sun, S. Endo, Y. Li, S. C. Benjamin, and X. Yuan, Variational algorithms for linear algebra, *Science Bulletin* **66**, 2181 (2021).
 - [4] C. Bravo-Prieto, R. LaRose, M. Cerezo, Y. Subasi, L. Cincio, and P. J. Coles, Variational quantum linear solver (2020), [arXiv:1909.05820 \[quant-ph\]](https://arxiv.org/abs/1909.05820).
 - [5] J. Preskill, Quantum computing in the NISQ era and beyond, *Quantum* **2**, 79 (2018).
 - [6] J. R. McClean, S. Boixo, V. N. Smelyanskiy, R. Babbush, and H. Neven, Barren plateaus in quantum neural network training landscapes, *Nature Communications* **9** (2018).
 - [7] H.-Y. Huang, K. Bharti, and P. Rebentrost, Near-term quantum algorithms for linear systems of equations with regression loss functions, *New Journal of Physics* **23**, 113021 (2021).
 - [8] E. Tang, A quantum-inspired classical algorithm for recommendation systems, in *Proceedings of the 51st Annual ACM SIGACT Symposium on Theory of Computing*, STOC 2019 (Association for Computing Machinery, New York, NY, USA, 2019) p. 217–228.
 - [9] N.-H. Chia, H.-H. Lin, and C. Wang, Quantum-inspired sublinear classical algorithms for solving low-rank linear systems (2018), [arXiv:1811.04852 \[cs.DS\]](https://arxiv.org/abs/1811.04852).
 - [10] A. Gilyén, S. Lloyd, and E. Tang, Quantum-inspired low-rank stochastic regression with logarithmic dependence on the dimension (2018), [arXiv:1811.04909 \[cs.DS\]](https://arxiv.org/abs/1811.04909).
 - [11] A. Gilyén, Z. Song, and E. Tang, An improved quantum-inspired algorithm for linear regression, *Quantum* **6**, 754 (2022).
 - [12] C. Shao and H. Xiang, Quantum circulant preconditioner for a linear system of equations, *Phys. Rev. A* **98**, 062321 (2018).
 - [13] Q. Zuo and T. Li, Fast and practical quantum-inspired classical algorithms for solving linear systems (2023), [arXiv:2307.06627 \[cs.DS\]](https://arxiv.org/abs/2307.06627).
 - [14] P. Davis, *Circulant Matrices* (Wiley, 1979).
 - [15] J. W. Cooley and J. W. Tukey, An algorithm for the machine calculation of complex Fourier series, *Mathematics of Computation* **19**, 297 (1965).
 - [16] M. Hestenes and E. Stiefel, Methods of conjugate gradients for solving linear systems, *Journal of Research of the National Bureau of Standards* **49**, 409 (1952).
 - [17] D. Coppersmith, An approximate Fourier transform useful in quantum factoring (1994), [arXiv:quant-ph/0201067 \[quant-ph\]](https://arxiv.org/abs/quant-ph/0201067).
 - [18] S. S. Zhou and J. B. Wang, Efficient quantum circuits for dense circulant and circulant like operators, *Royal Society Open Science* **4**, 160906 (2017).
 - [19] L.-C. Wan, C.-H. Yu, S.-J. Pan, F. Gao, Q.-Y. Wen, and S.-J. Qin, Asymptotic quantum algorithm for the Toeplitz systems, *Phys. Rev. A* **97**, 062322 (2018).

- [20] G. Brassard, P. Høyer, M. Mosca, and A. Tapp, Quantum amplitude amplification and estimation, in *Quantum computation and information*, Contemporary Mathematics, Vol. 305 (American Mathematical Society, Providence, RI, USA, 2002) pp. 53–74.
- [21] Y. Nam, Y. Su, and D. Maslov, Approximate quantum Fourier transform with $O(n \log(n))$ T gates, *npj Quantum Information* **6** (2020).
- [22] R. Cleve, A. Ekert, C. Macchiavello, and M. Mosca, Quantum algorithms revisited, *Proceedings of the Royal Society of London. Series A: Mathematical, Physical and Engineering Sciences* **454**, 339 (1998).
- [23] M. Özişik, H. Orlande, M. Colaço, and R. Cotta, *Finite Difference Methods in Heat Transfer* (CRC Press, 2017).
- [24] J. W. Thomas, *Numerical Partial Differential Equations: Finite Difference Methods* (Springer New York, 1995).
- [25] R. M. Gray, Toeplitz and circulant matrices: A review, *Foundations and Trends in Communications and Information Theory* **2**, 155 (2005).
- [26] M. Chen, On the solution of circulant linear systems, *SIAM Journal on Numerical Analysis* **24**, 668 (1987).
- [27] Y. Saad, Krylov subspace methods for solving large unsymmetric linear systems, *Mathematics of Computation* **37**, 105 (1981).
- [28] V. Simoncini and D. B. Szyld, Recent computational developments in Krylov subspace methods for linear systems, *Numerical Linear Algebra with Applications* **14**, 1 (2007).
- [29] S. Aaronson, Read the fine print, *Nature Physics* **11**, 291 (2015).
- [30] D. Koch, M. Samodurov, A. Projansky, and P. M. Alsing, Gate-based circuit designs for quantum adder inspired quantum random walks on superconducting qubits (2021), [arXiv:2012.10268 \[quant-ph\]](https://arxiv.org/abs/2012.10268).
- [31] T. G. Draper, Addition on a quantum computer (2000), [arXiv:quant-ph/0008033 \[quant-ph\]](https://arxiv.org/abs/quant-ph/0008033).
- [32] A. Y. Kitaev, Quantum measurements and the abelian stabilizer problem (1995), [arXiv:quant-ph/9511026 \[quant-ph\]](https://arxiv.org/abs/quant-ph/9511026).
- [33] E. Tang, Quantum principal component analysis only achieves an exponential speedup because of its state preparation assumptions, *Phys. Rev. Lett.* **127**, 060503 (2021).
- [34] N. M. Guseynov, A. A. Zhukov, W. V. Pogosov, and A. V. Lebedev, Depth analysis of variational quantum algorithms for the heat equation, *Phys. Rev. A* **107**, 052422 (2023).
- [35] E. Farhi, J. Goldstone, and S. Gutmann, A quantum approximate optimization algorithm (2014), [arXiv:1411.4028 \[quant-ph\]](https://arxiv.org/abs/1411.4028).
- [36] S. Hadfield, Z. Wang, B. O’Gorman, E. Rieffel, D. Venturelli, and R. Biswas, From the quantum approximate optimization algorithm to a quantum alternating operator ansatz, *Algorithms* **12**, 34 (2019).
- [37] A. M. Childs, R. Kothari, and R. D. Somma, Quantum algorithm for systems of linear equations with exponentially improved dependence on precision, *SIAM Journal on Computing* **46**, 1920 (2017).
- [38] M. Mosca and C. Zalka, Exact quantum Fourier transforms and discrete logarithm algorithms, *International Journal of Quantum Information* **02**, 91 (2004).
- [39] S. Aaronson, BQP and the polynomial hierarchy, in *Proceedings of the Forty-Second ACM Symposium on Theory of Computing*, STOC 2010 (Association for Computing Machinery, New York, NY, USA, 2010) p. 141–150.
- [40] S. Aaronson and A. Ambainis, Forrelation: A problem that optimally separates quantum from classical computing, *SIAM Journal on Computing* **47**, 982 (2018).